

# Learning Manipulation States and Actions for Efficient Non-prehensile Rearrangement Planning

Joshua A. Haustein<sup>1,†</sup>, Isac Arnekvist<sup>1,†</sup>, Johannes Stork<sup>1</sup>, Kaiyu Hang<sup>2</sup> and Danica Kragic<sup>1</sup>

**Abstract**—This paper addresses non-prehensile rearrangement planning problems where a robot is tasked to rearrange objects among obstacles on a planar surface. We present an efficient planning algorithm that is designed to impose few assumptions on the robot’s non-prehensile manipulation abilities and is simple to adapt to different robot embodiments. For this, we combine sampling-based motion planning with reinforcement learning and generative modeling. Our algorithm explores the composite configuration space of objects and robot as a search over robot actions, forward simulated in a physics model. This search is guided by a generative model that provides robot states from which an object can be transported towards a desired state, and a learned policy that provides corresponding robot actions. As an efficient generative model, we apply Generative Adversarial Networks. We implement and evaluate our approach for robots endowed with configuration spaces in  $SE(2)$ . We demonstrate empirically the efficacy of our algorithm design choices and observe more than 2x speedup in planning time on various test scenarios compared to a state-of-the-art approach.

## I. INTRODUCTION

In cluttered environments, a robot frequently encounters situations in which it needs to rearrange objects. A planning algorithm needs to reason about *which* objects to move, *where* to move them and *how* to move them. To achieve this, one needs to model the robot’s manipulation abilities and how these affect the environment. Many existing approaches simplify this by limiting manipulation to primitives like pick-and-place or straight-line pushing with the robot’s end-effector. Pushing is commonly further limited to a single object at a time and it is assumed that the object moves quasistatically, i.e. that inertial forces are neglectable and the object does not slide.

We are interested in enabling robots to utilize a wider range of non-prehensile manipulation skills. We aim to enable a robot to push multiple objects simultaneously with any of its parts and not just its end-effector. Modeling such skills explicitly, however, is labor-intensive and difficult to adjust to different robot embodiments and objects. Therefore, in this work, we devise an algorithm for planar non-prehensile rearrangement planning that does not require manually designed manipulation primitives.

Instead, our approach combines recent works on physics-based non-prehensile rearrangement planning [1]–[4] with re-

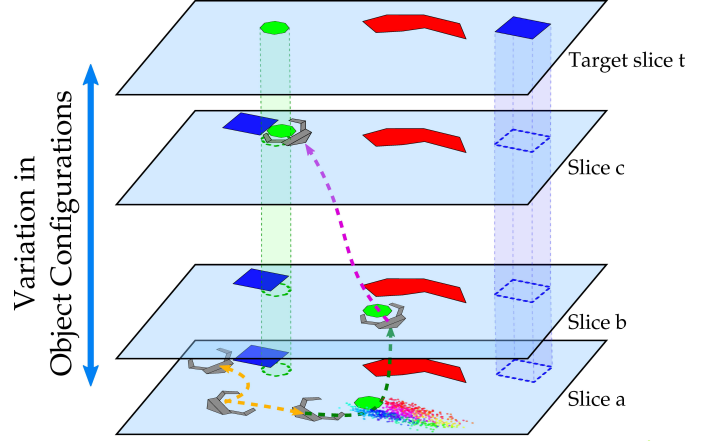


**Fig. 1:** Our planning algorithm rearranges movable objects on a plane (drawn in green and blue) in the presence of obstacles (red) using non-prehensile manipulation. The algorithm explores the composite configuration space of robot and objects in slices. Each slice corresponds to an object arrangement and is the subset of configurations with this arrangement.

**Slice a:** Configurations that lie within the same slice are connected through collision-free robot motions (yellow arrows). To purposefully transition towards a target slice  $t$ , our algorithm first selects an object (green) to transport towards the target. Thereafter, it samples a robot state from a learned distribution (colored points) from which the desired transport is feasible.

**Slice b:** After steering the robot to the sampled state, it applies a learned policy to push the object towards the target. The outcome of every robot action is modeled using a dynamic physics model, which also allows modeling unintended additional contact.

**Slice c:** The model also models object-object contact, which enables the approach to push multiple objects simultaneously.

**Video:** An illustrative video of this and additional supplementary material can be found on [https://joshuahaustein.github.io/learning\\_rearrangement\\_planning/](https://joshuahaustein.github.io/learning_rearrangement_planning/)

inforcement learning and generative modeling. Physics-based rearrangement planners explore the composite configuration space of objects and robot by performing a forward search over simple robot-centric actions. A physics model is applied to predict whether any action leads to collision and what the effects of this collision are. This allows the planner to exploit any manipulation the robot can achieve with its motions.

The key ideas of this work lie in augmenting this physics-based approach through the following concepts (see also Fig. 1):

1. We provide the algorithm with learned guidance on how to manipulate objects. For this, we train a generative model to efficiently produce samples from the set of robot configurations from which transporting an object towards a desired state is feasible. We achieve this by applying Generative Adversarial Networks (GANs). Additionally, we train a one-step policy that, once the robot is placed in such a configuration, provides object-specific pushing

<sup>1</sup> Robotics, Perception and Learning Lab (RPL), CAS, EECS, KTH Royal Institute of Technology, Stockholm, Sweden, E-mail: haustein, isacar, jastork, dani@kth.se

<sup>2</sup>GRAB Lab, Yale University, New Haven, USA, E-mail: kaiyu.hang@yale.edu

<sup>†</sup> J.A. Haustein and I. Arnekvist contributed equally to this work.

actions.

2. We structure the search by segmenting the search space into sets of configurations with similar object arrangements. This acknowledges that steering the robot is simpler than rearranging objects, and allows the algorithm to efficiently select suitable nearest neighbors for its search tree extension.

As a physics-based rearrangement planner, our approach can compute solutions where the robot pushes multiple objects simultaneously, as often as needed, and with any of its parts. In contrast to related approaches, our algorithm is more efficient and easily adapted to different object types and robot geometries.

We implement our approach for robots endowed with configuration spaces in  $SE(2)$ , and evaluate it experimentally. We observe the efficacy of our design choices and achieve more than 2x planning speedup compared to a state-of-the-art physics-based approach on various test scenarios.

The remainder of this work is structured as follows. First, we formalize the problem we address in Sec. II and summarize related works in Sec. III. Then, in Sec. IV we provide a more detailed overview of our concepts and contributions. We present the details of our approach in Sec. V, and evaluate it in Sec. VI. We discuss limitations and future work in Sec. VII.

## II. PROBLEM DEFINITION & NOTATION

We consider a rearrangement planning problem where a robot is tasked to rearrange multiple objects using only non-prehensile manipulation. The robot operates in a bounded environment that contains  $m$  movable objects among static obstacles  $\mathcal{O}$ . Its goal is to rearrange a target set  $\mathbf{T} \subseteq \{1, \dots, m\}$  of movable objects to some goal configurations  $\{g_i \mid i \in \mathbf{T}\}$ . This target set may either encompass all  $m$  objects or only a subset. To achieve its goal, the robot may manipulate any movable object while avoiding collisions with the static obstacles. We assume that all objects are rigid bodies that are placed on a single planar support surface and we disallow toppling over objects.

We formulate this problem as a motion planning problem on the composite configuration space of all movable objects and the robot,  $\mathcal{C}_{0:m} = \mathcal{C}_0 \times \dots \times \mathcal{C}_m$ . Here,  $\mathcal{C}_0$  is the configuration space of the robot and  $\mathcal{C}_i \subset SE(2)$  the configuration space of movable object  $i \in \{1, \dots, m\}$ . The composite configuration space is partitioned in free and obstacle space,  $\mathcal{C}_{0:m} = \mathcal{C}_{0:m}^{\text{free}} \cup \mathcal{C}_{0:m}^{\text{obst}}$ . We define the free space  $\mathcal{C}_{0:m}^{\text{free}}$  as the set of physically feasible configurations in which no two objects or the robot overlap and there is no collision with any static obstacle. Note that this definition includes configurations in which there is contact among movable objects or between these and the robot. For a composite configuration  $x = (x_0, \dots, x_m) \in \mathcal{C}_{0:m}$  we refer by  $x_i \in \mathcal{C}_i$  to the configuration of object  $i \geq 1$  and by  $x_0 \in \mathcal{C}_0$  to the configuration of the robot. We use the terms *state* and *configuration* interchangeably and distinguish between two different states using the superscript notation  $x^a, x^b$ . Our notation is summarized in Table I.

The robot can interact with its environment through actions  $u \in U$ . The purpose of our algorithm is to compute a

| Symbol  | Description  |
|---|--|
| $m$   | Total number of movable objects  |
| $\mathcal{O}$   | Static obstacles   |
| $\mathcal{C}_0$   | Configuration space of the robot   |
| $\mathcal{C}_i$   | Configuration space of object $i$  |
| $\mathcal{C}_{0:m}$   | Composite configuration space  |
| $\mathcal{C}_{1:m}$   | Space of all object arrangements   |
| $\mathcal{C}_{0:m}^{\text{free}}$   | Feasible configuration space   |
| $\mathcal{C}_{0:m}^{\text{obst}}$   | Obstacle space   |
| $x = (x_0, \dots, x_m)$   | Composite state  |
| $x_{1:m} = (x_1, \dots, x_m)$   | Composite state of objects   |
| $x^a, x^b$  | Two different composite states   |
| $x_i$   | State of object $i$  |
| $x_0$   | State of the robot   |
| $x_i^a, x_i^b$  | Two different states of object $i$   |
| $u \in U$   | Robot action in action space $U$   |
| $\mathbf{T} \subseteq \{1, \dots, m\}$  | Target object set  |
| $\mathcal{G} \subset \mathcal{C}_{0:m}^{\text{free}}$                           | Goal region  |
| $g_i \in \mathcal{C}_i$   | Goal configuration of object $i$   |
| $\xi : [0, t_{\max}] \rightarrow \mathcal{C}_{0:m}^{\text{free}}$               | Path in $\mathcal{C}_{0:m}^{\text{free}}$                                  |
| $\tau : [0, t_{\max}] \rightarrow U$  | Time-action mapping  |
| $d_{\mathcal{C}_i} : \mathcal{C}_i \times \mathcal{C}_i \rightarrow \mathbb{R}$ | Distance function on $\mathcal{C}_i$                                       |
| $\Gamma : \mathcal{C}_{0:m} \times U \rightarrow \mathcal{C}_{0:m}$             | Deterministic physics model  |
| $\perp$   | Empty value or invalid state   |
| $s$   | A subset of $\mathcal{C}_{0:m}$ (a slice) with the same object arrangement |
| $s_{1:m}$   | Object arrangement in slice $s$  |
| $s_i$   | Object $i$ 's state in slice $s$   |
| $d_s : \mathcal{C}_{1:m} \times \mathcal{C}_{1:m} \rightarrow \mathbb{R}$       | Distance function on $\mathcal{C}_{1:m}$                                   |
| $G_\varphi$   | Robot state generator  |
| $\pi_\theta$  | Pushing policy   |
| $L_\theta$  | Policy loss function   |
| $\mathcal{T}$   | Search tree of states in $\mathcal{C}_{0:m}^{\text{free}}$                 |
| $\mathcal{S}$   | Set of explored slices of $\mathcal{C}_{0:m}^{\text{free}}$                |
| $\nu_i$   | Physical properties of object $i$  |
| $x_i^d$   | Desired state for object $i$   |
| $x_i^j$   | Resulting state for object $i$   |

TABLE I: Notation used in this work.

time-action mapping  $\tau : [0, t_{\max}] \rightarrow U$  and a path  $\xi : [0, t_{\max}] \rightarrow \mathcal{C}_{0:m}^{\text{free}}$ , where  $t_{\max} \geq 0$  is the duration of this solution. The path  $\xi$  describes which states the system transitions through and the time-action mapping  $\tau$  which action to execute at time  $t \in [0, t_{\max}]$ . Such a pair  $(\xi, \tau)$  is physically feasible, if the non-holonomic constraint  $\xi(t) = f_{\text{physics}}(\xi(t), \tau(t))$  is fulfilled for all  $t \in [0, t_{\max}]$ . This constraint expresses the fact that objects do not move by themselves, but only as a result of forces exerted on them by the robot.

Given an initial state of the environment  $x^0 \in \mathcal{C}_{0:m}^{\text{free}}$  and a goal region  $\mathcal{G} \subseteq \mathcal{C}_{0:m}^{\text{free}}$ , the goal of our algorithm is to find a physically feasible tuple  $(\xi, \tau)$  such that  $\xi(0) = x^0$  and  $\xi(t_{\max}) \in \mathcal{G}$ . We define  $\mathcal{G} \subseteq \mathcal{C}_{0:m}^{\text{free}}$  as the set of states for which all target objects  $\mathbf{T}$  are located close to goal configurations  $g_i \in \mathcal{C}_i$ , i.e.

$$\mathcal{G} = \{x \in \mathcal{C}_{0:m}^{\text{free}} \mid \forall i \in \mathbf{T} : d_{\mathcal{C}_i}(x_i, g_i) \leq \epsilon_i\}$$

for some thresholds  $\epsilon_i > 0$  and distance functions  $d_{\mathcal{C}_i} : \mathcal{C}_i \times \mathcal{C}_i \rightarrow \mathbb{R}$ .

## III. RELATED WORKS

Our problem definition falls into the category of manipulation planning. Manipulation planning involves both planning

the motion of a robot and the manipulation of one or multiple objects in the presence of obstacles. Conceptually, we can distinguish between related works that focus on manipulating a single object from approaches that manipulate multiple objects. Manipulation planning for multiple objects can be further subdivided into manipulation planning among movable obstacles (MAMO) [5], [6], rearrangement planning (RP) [7]–[17] and navigation among movable obstacles (NAMO) [18]–[20].

These subcategories differ in the definition of the goal of the task. Applying our terminology, MAMO defines the target object set  $\mathbf{T}$ , or alternatively  $\mathcal{G}$ , to only encompass a single object. The remaining movable obstacles may need to be rearranged to succeed at the task, but their final configurations are not relevant. In contrast, in RP the target set  $\mathbf{T}$  encompasses all movable objects, i.e. the task is to rearrange all objects to specific locations. Finally, in NAMO the goal is to navigate the robot to a goal configuration when clearing the path from obstacles is required. In this case, the goal is only defined for the robot, i.e.  $\mathbf{T} = \{0\}$ , and the final configurations of the movable obstacles are not of interest.

Since we allow  $\mathbf{T}$  to be any subset of  $\{1, \dots, m\}$ , our problem covers manipulation planning for a single object, MAMO and RP, but not NAMO. Our work addresses the special cases of these problem classes when all objects are located on a single support surface and the robot only applies non-prehensile manipulation. For brevity, we refer to our problem simply as a rearrangement planning problem.

### A. Complexity and Concepts

Manipulation planning and in particular rearrangement planning is challenging. Wilfong et al. [7] showed that NAMO is NP-hard, and that rearrangement planning is PSPACE-hard. The complexity arises from the high dimensional search space and the constraint that objects only move as a consequence of the robot's actions. Alami et al. [8] therefore classify robot actions into two categories. *Transit* actions are collision-free robot motions, whereas *transfer* actions denote actions that manipulate objects. Planning *transit* actions is a classical robot motion planning problem, whereas planning *transfer* actions requires additional reasoning about the mechanics of manipulation.

Depending on the type of action, a manipulation planner operates on different lower dimensional subspaces of the configuration space  $\mathcal{C}_{0:m}$  [8], [21], [22]. If a robot moves without contact, it transitions between states within a subspace of  $\mathcal{C}_{0:m}^{\text{free}}$  for which all objects are at the same location. When, for instance, the robot grasps an object, it transitions to a different subspace, in which the grasped object and the robot move simultaneously. Other types of manipulation implicitly define different subspaces with different transition points. The challenges of manipulation planning lie within computing motions within each of these subspaces, finding transition points between them, as well as computing a global path that moves via multiple subspaces towards a goal.

### B. Manipulation Planning with Pick-And-Place

Many works on manipulation planning apply pick-and-place for *transfer* actions [5], [8], [10], [12]–[14], [22], [23]. From a planning perspective this is attractive for two reasons. First, it restricts where a transition from a *transit* to a *transfer* action can occur, i.e. at the configurations where the robot grasps a resting object. Second, it simplifies modeling how a state  $x = (x_0, \dots, x_m)$  evolves during a *transfer* action. Assuming the robot grasps object  $k$ , a pick-and-place operation moves  $x$  to  $x'$  such that only  $x_0 \neq x'_0$  and  $x_k \neq x'_k$ , while all other objects remain at the same location, i.e.  $x'_i = x_i$ . Furthermore, the new object state  $x'_k$  can be directly computed from the new robot state  $x'_0$  given a known transformation between the grasped object and the robot's end-effector's frame.

The early work by Alami et al. [8] presents two algorithms building on this. The first algorithm addresses rearrangement planning of multiple objects and assumes a finite set of grasps and placements. The second addresses manipulation planning for a single polygonal object under continuous grasps. Simeon et al. [22] adapted this approach to manipulation planning for a single object under continuous grasps and placements using probabilistic roadmaps.

Later, Stilman et al. [5] addressed the problem of MAMO using pick-and-place. The algorithm first computes which objects collide with the desired pick-and-place operation on the target object and then recursively attempts to clear these obstructions. To limit the recursion depth, the approach assumes *monotone* problems, where each obstructing object needs to be moved at most once.

Krontiris et al. [12] integrate a modification of this MAMO algorithm as local planner into a bidirectional RRT algorithm [24] to solve rearrangement problems. The RRT algorithm explores the space of object arrangements and utilizes the MAMO algorithm to compute pick-and-place sequences to transition between different arrangements. More recently [13], the same authors augmented this approach using minimal constraint removal paths [25] to compute an order in which to move the objects that minimizes obstructions, thus avoiding the extensive backtracking of the original MAMO algorithm. This results in a non-monotone rearrangement planning algorithm that was demonstrated to solve even challenging problems with many objects efficiently.

### C. Manipulation Planning with Diverse Manipulation Types

A robot can rearrange objects more effectively and efficiently when it is not only limited to pick-and-place, but can also apply non-prehensile manipulation like pushing. Pushing is useful as it is faster to execute, can reduce uncertainty [26] and can be applied to heavy or multiple objects simultaneously. Hence, several existing works aim at combining diverse types of manipulation [6], [15]–[17], [27] in a single planner.

In these works, the different types of manipulation are abstracted as manipulation primitives. A manipulation primitive defines what its preconditions and effects are. For instance, for a picking primitive the precondition is that the robot's end effector is located at a grasp pose relative to a target object. Its effect is then, as described above, the change of a single

object's pose and the robot's configuration. Similarly, one can formalize primitives for pushing. Here, however, in general both the preconditions and effects are more challenging to model. A robot may push an object  $k$  with its various parts from many different robot configurations. Furthermore, the pushed object may slide or collide with other objects, resulting in state changes for these as well. This renders modeling the resulting state  $x'$  of a pushing operation challenging.

To simplify this, the works in this category commonly limit the implemented pushing primitives to cases where a single object is pushed with the robot's end-effector. The effect of pushing is often assumed to be simply the translation of the robot's end-effector applied to the pushed object.

More sophisticated pushing primitives are presented by Dogar et al. [6]. The authors apply a quasistatic pushing model [28] to compute capture regions of different pushing primitives. These capture regions describe sets of object poses relative to a robot link, e.g. the palm of a robotic hand. If an object is located within the capture region of a primitive, it is guaranteed to end up inside a known subregion of this region once the primitive was executed. This allows to compute solutions for MAMO under object pose uncertainty, but is limited by the quasistatic assumption that inertial forces are negligible. Furthermore, the approach is limited to manipulating a single object at a time.

#### D. Manipulation Planning with Pushing

There have also been works that solely focus on manipulation planning for pushing [28]–[30]. Lynch et al. [28] studied the controllability of a single object pushed with point or line contacts under the quasistatic assumption. The authors present a planner based on Dijkstra's algorithm to plan pushing a single object among static obstacles using stable line contacts that can be executed open-loop. More recently, Zhou et al. [30] showed that quasistatic push planning of an object using a single contact can be reduced to computing a Dubins path. The authors applied this in the RRT algorithm to plan pushing paths that avoid obstacles with the pusher and the object. While these approaches produce very accurate solutions that can be executed open-loop, they are limited to situations where the quasistatic assumption holds and only a single object is pushed.

In rearrangement planning it may be more efficient to push multiple objects simultaneously than in sequence. Ben-Shahar et al. [9], [21] present a rearrangement planner that, in principle, allows pushing objects simultaneously. The approach performs a hill-climbing search on a grid-discretization of the composite configuration space. The search minimizes a cost function that denotes the minimal cost to reach the goal. This cost is precomputed on the discrete search space using a reverse pushing model that could take object-object contacts and non-quasistatic physics into account. Obtaining such a general reverse pushing model, however, is difficult and the authors present only a simplified model in their experiments.

1) *Integrating a Physics Model:* Over the last decades rigid-body physics simulators have become widely available [31]–[34]. These simulators can model the physical

interactions between a robot and its surrounding objects. Integrating such a physics model with a motion planning algorithm allows to predict the effects of robot actions.

Zito et al. [35] use this approach to plan to push a single object. Kitaev et al. [36] combine a physics model with stochastic trajectory optimization to compute grasp approach motions in clutter. A similar idea has been applied to rearrangement planning and MAMO in [2] and [3]. These works integrate a physics model into the kinodynamic RRT algorithm [37]. In [2], a quasistatic multi-body pushing model is used to generate solutions where the robot utilizes its full-arm to push multiple object simultaneously. In [3], instead a dynamic physics model is used that allows generating solutions where a robot pushes and thrusts sliding objects into place.

In both [2] and [3] the RRT algorithm explores  $\mathcal{C}_{0:m}$  by forward propagating randomly selected robot actions through the physics model. These robot-centric actions move the robot and make no explicit assumption on how an object may be manipulated. As a consequence, both approaches can achieve a diverse set of manipulation actions, but suffer from a poor exploration of the search space. Consider two states  $x^a, x^b \in \mathcal{C}_{0:m}$  for which some object state differs, i.e.  $x_k^a \neq x_k^b$  for an object  $k$ . Without any object-centric pushing primitives, the algorithms lack guidance on how to select an action that takes the search from  $x^a$  closer to  $x^b$ . Randomly sampling robot-centric actions may lead to incidental contact with an object, but it is very unlikely to sample an action that moves the object towards the desired state. This diminishes the RRT's property of rapidly exploring the search space.

King et al. [4] address this by augmenting the approach from [2] with object-centric pushing primitives. These primitives are similar to the ones described in Sec. III-C, but their effects are modeled using the physics model. This in combination with random robot-centric actions significantly improves the algorithm's performance. However, designing these primitives manually still poses a limiting factor. First, providing the algorithm with diverse primitives such as pushing with the elbow, or pushing with the forearm is labor-intensive. Second, adapting the planner to a different robot generally requires the human designer to create new primitives. Third, selecting the most suitable primitive within the planner efficiently becomes challenging for a large set of primitives.

2) *Learning for Pushing:* An alternative to modeling pushing analytically is to apply machine learning. The works by Scholz et al. [11] and Elliot et al. [38] learn probabilistic forward models for manually designed manipulation primitives to rearrange objects. As these forward models are learned from the real world, the approaches make few assumptions on the outcome of the physical interactions. Object-to-object contacts, however, are not modeled. Furthermore, the use of manipulation primitives limits the type of contact the robot applies.

Another probabilistic model-based approach was proposed by Wang et al. [39] and addresses push planning for a single object under uncertainty. The authors propose to first learn a distribution of stochastic pushing outcomes in a world containing no obstacles. Then, given the task to push the object to some goal in the presence of obstacles, the approach

first constructs several search trees of collision-free object poses using the RRT algorithm. The nodes of these search trees are then treated as the states of a finite state Markov decision process (MDP), where the transition probabilities are given by the pushing distribution learned beforehand. In this MDP, an optimal value function and policy are then computed iteratively to solve the given problem. This approach has the benefit that the learned pushing policy is robust against uncertainty. Also, being model-based reduces the amount of data needed to train the policy [40]. The approach, however, does not address how to plan the motion of the robot, and instead assumes that the robot can always transition to any pose relative to the object. Besides, the value function and policy are based on a dynamics model which is only valid for the single trained object. Pushing a different object requires learning a new model.

To remove restrictions on the type of contact, and the type of objects, Finn et al. [41] present an end-to-end approach for pushing. Instead of explicitly modeling the manipulated object, the approach learns probabilities of how pixels move in a camera image as a result of robot actions. These learned probability distributions are, however, only informative for short time scales, and are unlikely to generalize to longer time-scales and planning in complex scenes.

In contrast to these model-based approaches, Andrychowicz et al. [42] apply Q-learning to learn a policy for pushing a single object in an obstacle-free environment. As the previously mentioned works [41] and [39], this makes few to no assumptions on the type of contact. Being model-free also means that the dependence on a correct approximation of the dynamics is no longer needed. Any changes to the environment or the pushed object, however, requires training the policy from scratch again.

#### E. Our Approach

The goals of this work are to devise an algorithm that

- computes solutions to the problem defined in Sec. II,
- makes few limiting assumptions on how the robot can manipulate objects,
- maintains planning efficiency.

The ideas from [2] and [3] address the first two goals by integrating a physics model into the kinodynamic RRT algorithm. Both approaches, however, suffer from a poor exploration rate, which leads to long planning times. King et al. [4] demonstrated how the efficiency of this family of algorithms can be improved by equipping them with object-centric actions. The proposed action primitives, however, require a human designer and thus reintroduce limiting assumptions on the robot's manipulation abilities. The learning-based approaches presented in Sec. III-D2 either also require some primitives or do not allow manipulating multiple objects at a time.

### IV. CONCEPT AND CONTRIBUTIONS

As stated in Sec. I, we adopt the ideas from [2]–[4]. Similar to these works, we present a sampling-based planning algorithm that explores the composite configuration space  $\mathcal{C}_{0:m}$  as a forward search over simple robot-centric actions  $u \in U$ .

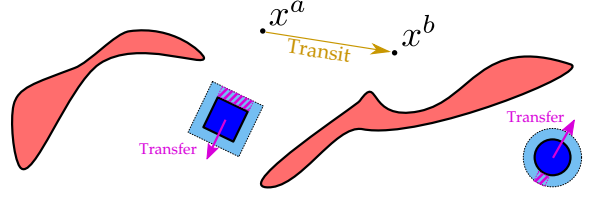


**Fig. 2:** An illustration of a slice of the configuration space  $\mathcal{C}_{0:2}$  for a fixed object arrangement for a point robot. The red areas show parts of  $\mathcal{C}_{0:2}^{\text{obs}}$  that are inaccessible due to collisions with static obstacles. The dark blue areas show parts that are in collision with movable objects. The yellow arrow indicates a collision-free *transit* movement between two states  $x^a, x^b$ . The light blue areas show subsets of  $\mathcal{C}_{0:2}$  from which pushing the objects, i.e. a *transfer* action, is possible given a particular action space  $U$ . If we intend to push an object in some desired direction (pink arrows), these subsets are further restricted (pink striped areas).

To predict the outcome of these actions, we apply a dynamic physics model  $\Gamma$ . This, on the one hand, guarantees that the algorithm computes physically feasible solutions. On the other hand, it shifts the assumptions on the effects of the actions from the algorithm to the model. For instance, using a dynamic physics simulator as a model allows our approach to compute solutions where the robot manipulates rolling or sliding objects, or exploits object-to-object contacts.

In order to avoid planning in a state space that includes velocities, however, we follow the approach from [3] and limit our search to sequences of dynamic actions between statically stable states. This means that all objects and the robot are required to come to rest after each action within some time limit. Formally, we assume the physics model  $\Gamma$  to be a function  $\Gamma : \mathcal{C}_{0:m}^{\text{free}} \times U \rightarrow \mathcal{C}_{0:m}^{\text{free}} \cup \perp$  that maps a configuration  $x \in \mathcal{C}_{0:m}^{\text{free}}$  and an action  $u$  to the resulting state  $\Gamma(x, u) = x' \in \mathcal{C}_{0:m}^{\text{free}}$  of this action, or a special value  $\perp$ , if the action leads to an invalid, i.e. non-resting, state.

We augment this physics-based search through two key concepts. First, we provide the algorithm with guidance on how to achieve *transfer* actions using machine learning. This enables our algorithm to compute object-centric actions without manually designed primitives. Second, we segment the search space  $\mathcal{C}_{0:m}$ , and accordingly the search tree, in sets with similar object arrangements. This structures the search and results in a more efficient exploration of  $\mathcal{C}_{0:m}$  than by the RRT algorithms in [2]–[4].

To illustrate these concepts, consider Fig. 2. It shows an illustration of a cross section of the configuration space  $\mathcal{C}_{0:2}$  for a holonomic point robot and  $m = 2$  objects. We refer to such a cross section of states  $\{x \in \mathcal{C}_{0:m} | x_{1:m} = x_{1:m}^f\}$  with a fixed object arrangement  $x_{1:m}^f = (x_1^f, \dots, x_m^f)$  as slice of  $\mathcal{C}_{0:m}$ . Navigating a robot within a slice, i.e. performing *transit* actions, is a classical motion planning problem that is well studied [24]. In particular, steering the robot between two states  $x^a = (x_0^a, x_1^f, \dots, x_m^f)$ ,  $x^b = (x_0^b, x_1^f, \dots, x_m^f)$  within the same slice ignoring obstacles is simple for many types of robots. Navigating to a different slice, i.e. performing *transfer* actions, however, requires the robot to manipulate objects.

The set of robot configurations from which this is achievable within one action  $u \in U$  is shown in Fig. 2 in light blue. This set is further restricted, if we intend to push an object in a particular direction (pink regions). We refer to these states as



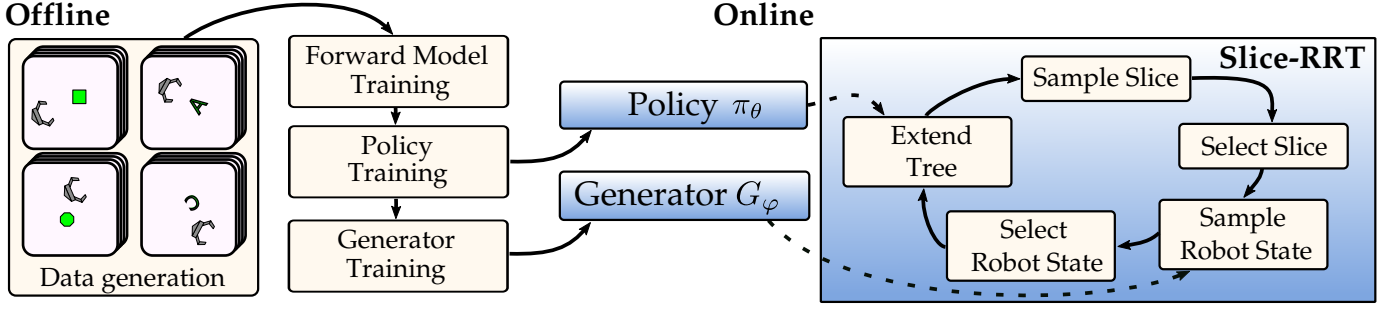


**Fig. 3:** Our approach consists of an offline and online phase. In the offline phase, a policy  $\pi_\theta$  and a state generator  $G_\varphi$  are learned from data generated with a physics model. The generator provides samples of robot states that allow transporting an object towards a desired state with a single action. The policy provides such robot actions. Online, we apply a modified version of the RRT algorithm to search for a rearrangement solution. The algorithm explores the search space in slices of similar object arrangements. To purposefully transition between different slices, it applies the policy and generator to push objects towards target states.

manipulation states.

The shape of the set of manipulation states depends on the shape of the object, the action space  $U$ , and the robot’s geometry. Rather than approximating this manually through primitives, we train a generative model to produce samples of manipulation states. In order to transport an object to a desired state, our algorithm then first steers the robot to such a sampled manipulation state. Then, once the robot is placed in a manipulation state, the algorithm selects an action  $u \in U$  to transport the object towards the desired state.

Selecting this action is generally also non-trivial. The most suitable action depends on physical properties of the object and the state of the robot. Hence, we additionally train a policy to provide this action to the planner. With these two components in place, our algorithm proceeds as illustrated in Fig. 1 and explores  $\mathcal{C}_{0:m}$  slice-by-slice.

To summarize, the contributions of this work are:

1. An efficient sampling-based algorithm for rearrangement planning that is agnostic to the details of manipulation.
2. An approach to learn manipulation states and actions using reinforcement learning and Generative Adversarial Networks (GANs).
3. An implementation and evaluation of this framework for robots endowed with configuration spaces in  $SE(2)$ .

## V. METHOD

An overview of our approach is shown in Fig. 3. It consists of three key components: the planning algorithm, the generative model  $G_\varphi$  and the pushing policy  $\pi_\theta$ . The planner computes a solution for an instance of our problem when queried online. Both the policy and the generator are trained offline and parameterized so that they can be applied to objects of different shape, mass and friction properties.

### A. Planning Algorithm

The planning algorithm is outlined in Algorithm 1. We first provide a high-level overview of this algorithm and then describe the details of its subroutines in the following subsections.

#### Algorithm 1: The rearrangement planning algorithm.

---

**Input:** Start configuration  $x^0 \in \mathcal{C}_{0:m}^{\text{free}}$ , maximum number of iterations  $n_{\max}$ , goal region  $\mathcal{G} \subset \mathcal{C}_{0:m}^{\text{free}}$   
**Output:** Solution  $[(x^0, u^0), \dots, (x^n, \perp)]$  or  $\emptyset$

```

1  $s^0 \leftarrow \text{SLICE}(x^0)$  // Obtain the slice that  $x^0$  lies in
2  $\mathcal{S} \leftarrow \{s^0\}$  // Set of all explored slices
3  $\mathcal{T} \leftarrow \text{TREE}(x^0)$  // Tree of explored states
4 for  $j \leftarrow 1, \dots, n_{\max}$  do
5    $s^d \leftarrow \text{SAMPLESLICE}()$ 
6    $s^j \leftarrow \arg \min_{s \in \mathcal{S}} d_s(s, s^d)$  // Closest explored slice
7    $t \leftarrow \text{RANDOMCHOICE}(\{0\} \cup \{1, \dots, m\})$ 
8   if  $t = 0$  then
9      $x_0^d \leftarrow \text{SAMPLEUNIFORM}(\mathcal{C}_0^{\text{free}})$ 
10  else
11     $x_0^d \leftarrow \text{QUERYGENERATOR}(s^j, s^d, t)$ 
12   $x^j \leftarrow \arg \min_{x \in s^j} d_{C_0}(x_0, x_0^d)$  // Closest state in  $s^j$ 
13   $x^d \leftarrow (x_0^d, s_1^d, \dots, s_m^d)$  // Constructed target state
14   $\mathcal{T}, \mathcal{S} \leftarrow \text{EXTENDTREE}(x^j, x^d, t, \mathcal{T}, \mathcal{S})$ 
15  if  $\mathcal{T} \cap \mathcal{G} \neq \emptyset$  then
16    return  $\text{EXTRACTANDSHORTCUT}(\mathcal{T})$ 
17 return  $\emptyset$ 

```

---

1) *Overview:* Given a start state  $x^0 \in \mathcal{C}_{0:m}^{\text{free}}$ , the algorithm starts with initializing its search tree  $\mathcal{T}$  and a set  $\mathcal{S}$ , which keeps track of the slices of  $\mathcal{C}_{0:m}^{\text{free}}$  that the explored states in  $\mathcal{T}$  lie in. It then iteratively grows the search tree  $\mathcal{T}$  on  $\mathcal{C}_{0:m}^{\text{free}}$  in a similar fashion to the kinodynamic RRT algorithm until it either adds a goal state  $g \in \mathcal{G}$  to the tree or a maximum number of iterations  $n_{\max}$  is reached.

In each iteration the algorithm needs to select where to extend its search tree from. For this, it first randomly samples a slice  $s^d$  by sampling a random object arrangement. Next, it selects the explored slice  $s^j \in \mathcal{S}$  that is closest to  $s^d$  w.r.t. some distance function  $d_s$ . For the tree extension the algorithm will either attempt to perform a *transit* action within the selected slice  $s^j$  or a *transfer* action towards the sampled slice  $s^d$ . To decide this, it randomly chooses an index  $t \in \{0, \dots, m\}$ . In case it chooses the robot,  $t = 0$ , the algorithm will attempt a *transit* action and uniformly samples a robot state  $x_0^d$  as a goal for this transit. In case it chooses an object,  $t \in \{1, \dots, m\}$ , it samples a robot state  $x_0^d$  that likely allows it to push object  $t$  from its state  $s_t^j$  in the current

selected slice to its state  $s_t^d$  in the randomly sampled slice. For this, it applies the generator  $G_\varphi$  that is described in more detail later.

In both cases, the algorithm then needs to select an actual composite state  $x^j \in \mathcal{T}$  from the search tree  $\mathcal{T}$  to extend from. Since it already selected the slice  $s^j$  for extension, it only needs to search for this state within this slice. For this, it searches for the state  $x^j \in \mathcal{T} \cap s^j$  that minimizes the robot state distance  $d_{C_0}$  to the sampled robot state  $x_0^d$ . Depending on the choice of  $t$ , the extend function EXTENDTREE will then either simply steer the robot to  $x_0^d$ , or additionally attempt to push object  $t$  towards  $x_t^d$  using the policy  $\pi_\theta$ .

The above proceeds until the loop is terminated. If a goal state  $g \in \mathcal{G}$  was added to the tree, the algorithm returns a solution  $(\xi, \tau)$  represented as sequence of state and action tuples  $\{(x^j, u^j)\}_{j=0}^n$  with  $x^n = g$ . Each state in this solution  $x^{j+1} = \Gamma(x^j, u^j)$  is the physical outcome of the previous action applied to the previous state. If the algorithm failed to add a goal within  $n_{\max}$  iterations, a special value  $\emptyset$  is returned to indicate failure.

2) *Sampling*: Each iteration starts with the SAMPLESLICE function, which samples a slice by sampling an object arrangement. This is done by either uniformly sampling the space of object arrangements  $\mathcal{C}_{1:m}$ , or with some probability  $p_g$ , by sampling the set of goal arrangements in  $\mathcal{G}$ . Similarly, the function RANDOMCHOICE samples an index  $t \in \{0, 1, \dots, m\}$  with bias towards either the robot  $t = 0$  or a target object  $t \in \mathbf{T}$ .

3) *Selecting Nearest Neighbors*: To select the nearest explored slice  $s^j \in \mathcal{S}$ , we require a distance function  $d_s$ . Measuring this distance, however, is challenging. Ideally, we would apply a distance function that expresses a minimal cost that it takes the robot to move all objects from one slice to the other. Such a cost, however, is generally not available, as it would require to take all robot motions needed to clear occlusions as well as simultaneous object manipulation into account. Instead, we opt to approximate this through the distance function

$$d_s(s^a, s^b) = \sum_{i=1}^m d_{C_i}(s_i^a, s_i^b). \quad (1)$$

that sums the distances of the individual object states.

4) *Extending the Tree*: In the EXTENDTREE function, Algorithm 2, the search tree is either extended using a targeted extension strategy or with some small probability  $p_{rand}$  by a random action. When following our strategy, it first uses a steering function for the robot to compute an action  $u_0$  that attempts to move the robot from its current state  $x_0^j$  towards the sampled state  $x_0^d$ . This action is then forward propagated in the subroutine EXTENDSTEP using the physics model  $\Gamma$ . If this action leads to a valid state, the EXTENDSTEP function adds the resulting state to the tree  $\mathcal{T}$  and updates  $\mathcal{S}$  accordingly. Note that although this action is intended to move only the robot, it may result in collision and thus also move any of the  $m$  movable objects. The EXTENDSTEP function therefore returns the resulting composite state  $x^c = \Gamma(x^j, u_0)$ .

If  $t$  is not the robot,  $x_0^d$  is a manipulation state provided by our generator to push object  $t$ . Hence, the algorithm

---

**Algorithm 2:** The EXTENDTREE function

---

**Input:** Object identifier  $t$ , current tree node  $x^j \in \mathcal{T}$  to extend, state to extend towards  $x^d \in \mathcal{C}_{0:m}$ , search tree  $\mathcal{T}$ , explored slices  $\mathcal{S}$   
**Constants:**  $p_{rand} \in [0, 1]$   
**Output:** Updated  $\mathcal{T}$  and  $\mathcal{S}$

```

1 if UNIFORM( $[0, 1]$ )  $\leq p_{rand}$  then
2    $u \leftarrow \text{UNIFORM}(U)$ 
3    $\perp, \perp, \mathcal{T}, \mathcal{S} \leftarrow \text{EXTENDSTEP}(x^j, u, \mathcal{T}, \mathcal{S})$ 
4 else
5    $u_0 \leftarrow \text{STEER}(x_0^j, x_0^d)$ 
6    $\text{valid}, x^c, \mathcal{T}, \mathcal{S} \leftarrow \text{EXTENDSTEP}(x^j, u_0, \mathcal{T}, \mathcal{S})$ 
7   if not  $\text{valid}$  or  $t \neq r$  then
8     return  $\mathcal{T}, \mathcal{S}$ 
9    $u \leftarrow \text{QUERYPOLICY}(x_0^c, x_t^c, x_t^d)$ 
10   $\perp, \perp, \mathcal{T}, \mathcal{S} \leftarrow \text{EXTENDSTEP}(x^c, u, \mathcal{T}, \mathcal{S})$ 
11 return  $\mathcal{T}, \mathcal{S}$ 
```

---

next queries the policy  $\pi_\theta$  in QUERYPOLICY to achieve the desired push. The returned action is then again passed to the EXTENDSTEP function and  $\mathcal{T}$  and  $\mathcal{S}$  are updated accordingly.

5) *Physics Propagation*: Given a state  $x \in \mathcal{C}_{0:m}^{\text{free}}$  the EXTENDSTEP function forward propagates an action  $u$  through the physics model  $\Gamma$ . An action is considered invalid, if the scene fails to come to rest within some time limit, i.e.  $\Gamma(x, u) = \perp$ , or if the action leads to collisions of either the robot or any movable object with static obstacles. Collisions between movable objects, in contrast, are allowed and modeled accordingly. If the propagation is valid and  $x' = \Gamma(x, u)$  is within bounds, the search tree  $\mathcal{T}$  and  $\mathcal{S}$  are updated accordingly.

6) *Extracting and Shortcutting the Path*: If the algorithm succeeds at adding a goal state to the tree, the function EXTRACTANDSHORTCUT extracts the solution  $(x^0, u^0), \dots, (x^n, \perp)$  with  $x^n \in \mathcal{G}$  from  $\mathcal{T}$ . Due to the randomization of the algorithm, this solution may contain multiple actions that are not required. We shortcut these using the shortcut algorithm presented by King et. al [2]. The algorithm selects two pairs  $(x^i, u^i), (x^j, u^j)$  and replaces  $u^i$  with an action moving the robot from state  $x_0^i$  to  $x_0^j$ . Thereafter, it forward propagates this new action and all remaining actions  $u^k$  with  $j \leq k < n$  through the physics model to probe whether the goal can still be achieved. If this is the case and the resulting solution is shorter in terms of execution time, the old solution is replaced by the new one. This process is repeated until either all pairs have been attempted or a timeout occurred. The pairs can be selected in different orders, although uniform random sampling performed best in our experiments.

## B. Learning the Policy and the Generator

The QUERYGENERATOR and QUERYPOLICY functions provide the planner with a manipulation state and an action to transport a single object  $i$  from a state  $x_i$  to some desired state  $x_i^d$ . As illustrated in Sec. IV, there might be multiple such manipulation states that the generator could sample. Similarly, in general there are several actions that the policy

could select to achieve the *transfer*. We can represent these two sets implicitly through two families of distributions

$$p(x_0|x_i^d, x_{1:m}, \nu_{0:m}, \mathcal{O}), \quad (2)$$

$$p(u|x_i^d, x_{0:m}, \nu_{0:m}, \mathcal{O}) \quad (3)$$

that place all probability mass on the manipulation states and actions for the desired object transport. Both types of distributions are conditioned on the state of all objects  $x_{1:m}$ , physical properties of the objects and the robot  $\nu_{0:m}$ , and all static obstacles  $\mathcal{O}$ . The action distributions in Eq. (3) are additionally conditioned on the state of the robot  $x_0$ .

With this representation, learning the generator and the policy could be achieved by learning parameters  $\theta$  and  $\phi$  that characterize instances from these families of distributions. Once learned, the generator and the policy could then produce the desired samples by sampling from these distributions. Learning  $\theta$  and  $\phi$  for this general case, however, is very difficult. The learned distributions would need to be conditioned on an arbitrary number of movable objects  $m$  as well as all possible static obstacle configurations  $\mathcal{O}$ .

Therefore, instead, we simplify the problem to learning distributions of the form

$$p(x_0|x_i^d, x_i, \nu_i), \quad (4)$$

$$p(u|x_i^d, x_0, x_i, \nu_i). \quad (5)$$

In other words, we choose to learn the generator and the policy in an obstacle-free world containing only the robot and a single object. We leave it to the planning algorithm to find manipulation states and actions that are feasible in the full problem. Also, we learn both policy and generator for a single robot at a time. Applying the planner to a different robot requires training a different policy and generator. For brevity, we thus omit the dependency on the robot's physical properties  $\nu_0$ .

In the following, we first present how we learn the policy, i.e. an instance of an action distribution, from data generated offline. Thereafter, we derive an instance of a manipulation state distribution from this policy and present how the generator can be trained to efficiently sample from this distribution within the planner.

1) *Learning the Policy*: The parameter  $\theta$  that characterizes the policy can be found by solving the problem

$$\min_{\theta} \mathbb{E}_{x_0, x_i^d, x_i, \nu_i} [\mathbb{E}_{x'_i, u} [d_{\mathcal{C}_i}(x'_i, x_i^d) \mid x_0, x_i^d, x_i, \nu_i, \theta]] \quad (6)$$

over some training distributions for  $x_0, x_i^d, x_i, \nu_i$ . The inner expected value

$$\begin{aligned} \mathbb{E}_{x'_i, u} [d_{\mathcal{C}_i}(x'_i, x_i^d) \mid x_0, x_i^d, x_i, \nu_i, \theta] = \\ \iint d_{\mathcal{C}_i}(x'_i, x_i^d) p(x'_i \mid u, x_0, x_i, \nu_i) dx'_i \\ p(u \mid x_i^d, x_0, x_i, \nu_i, \theta) du \end{aligned} \quad (7)$$

is the expected distance between a desired object state  $x_i^d$  and the actual state  $x'_i$  that the policy parameterized by  $\theta$  achieves, given it is executed when the robot is in state  $x_0$  and the object with properties  $\nu_i$  is in state  $x_i$ . The successor state distribution  $p(x'_i \mid u, x_0, x_i, \nu_i)$  describes the physical outcome of an action.

Although we could model this using the deterministic physics model  $\Gamma$ , it proves useful to apply a non-deterministic model for learning the policy. We will motivate this shortly.

We simplify the expression in Eq. (7) by choosing our policy to be a deterministic function  $u_{\theta} := \pi_{\theta}(x_0, x_i, x_i^d, \nu_i)$ . In other words, we enforce the action distribution to be a Dirac delta function  $p(u \mid x_i^d, x_0, x_i, \nu_i, \theta) = \delta(u - \pi_{\theta}(x_0, x_i, x_i^d, \nu_i))$ . With this, the expected distance in Eq. (7) reduces to

$$\begin{aligned} L_{\theta}(x_0, x_i, x_i^d, \nu_i) &:= \int d(x'_i, x_i^d) p(x'_i \mid u_{\theta}, x_0, x_i, \nu_i) dx'_i \\ &= \mathbb{E}_{x'_i} [d_{\mathcal{C}_i}(x'_i, x_i^d) \mid u_{\theta}, x_0, x_i, \nu_i] \end{aligned} \quad (8)$$

and our problem of learning the policy becomes

$$\min_{\theta} \mathbb{E}_{x_0, x_i^d, x_i, \nu_i} [L_{\theta}(x_0, x_i, x_i^d, \nu_i)]. \quad (9)$$

To solve this problem efficiently, we need to have access to the gradient of the loss  $L_{\theta}(x_0, x_i, x_i^d, \nu_i)$  w.r.t.  $\theta$ . To acquire this, we choose the distance function on  $\mathcal{C}_i \subseteq SE(2)$  to be of the form  $d_{\mathcal{C}_i}(x'_i, x_i^d) = \sum_{j=1}^3 \sigma_j (x'_{ij} - x_{ij}^d)^2$  with positive weights  $\{\sigma_j\}_{j=1}^3$ . The loss then becomes

$$L_{\theta}(x_0, x_i, x_i^d, \nu_i) = \sum_{j=1}^3 \sigma_j \mathbb{E}_{x'_i} [(x'_{ij} - x_{ij}^d)^2 \mid u_{\theta}, x_0, x_i, \nu_i], \quad (10)$$

where  $x_{i0}, x_{i1} \in \mathbb{R}$  denote the object's position and  $x_{i2} \in SO(2)$  its orientation. Expanding the square and rewriting yields

$$\begin{aligned} L_{\theta}(x_0, x_i, x_i^d, \nu_i) = \\ \sum_{j=1}^3 \sigma_j \left( \text{Var}_{x'_i} [x'_{ij}] + (\mathbb{E}_{x'_i} [x'_{ij}] - x_{ij}^d)^2 \right), \end{aligned} \quad (11)$$

where both variance and expected value are conditioned on  $x_0, x_i, \nu_i, u_{\theta}$ .

This means we can express the loss  $L_{\theta}$  as a function of forward models

$$f_{\mu}(x_0, x_i, \nu_i, u) = \mathbb{E}_{x'_i} [x'_i \mid x_0, x_i, \nu_i, u] \quad (12)$$

and

$$f_{\sigma^2}(x_0, x_i, \nu_i, u) = \text{Var}_{x'_i} (x'_i \mid x_0, x_i, \nu_i, u). \quad (13)$$

In particular, if these forward models are differentiable w.r.t. to the action argument  $u$ , we can apply the chain rule in Eq. (11) to obtain the gradient of  $L_{\theta}$  w.r.t.  $\theta$ . With this deterministic policy gradient [43] we can then learn the policy by solving Eq. (9).

We can obtain differentiable models  $f_{\mu}$  and  $f_{\sigma^2}$  through supervised learning from a data set  $\{(x_0^j, x_i^j, \nu_i^j, u^j, (x'_i)^j) \mid j \in \mathbb{N}\}$  of robot-object interactions. We generate this data set offline using the physics model  $\Gamma$ . Learning the models  $f_{\mu}$  and  $f_{\sigma^2}$  in this way has the advantage that we are free in choosing any physics model  $\Gamma$  for generating the data. In particular, this allows us to choose models  $\Gamma$  for which gradients w.r.t.  $u$  are not available, as it is the case for many rigid body physics simulators.

Eq. (11) also provides insight into why we choose to apply a non-deterministic physics model for learning the policy.



If we applied a deterministic model, i.e. the successor state distribution  $p(x'_i|u, x_0, x_i, \nu_i)$  had zero-variance, the variance term in Eq. (11) would disappear. Hence, our policy could select any action  $u \in U$  for a state  $(x_0, x_i)$  that transports the object as close as possible to  $x_i^d$ . Not all of these actions, however, are equally desirable in practice. For instance, a robotic hand pushing an object with the tip of its finger only works reliably if the object behaves exactly as predicted by the physics model. Pushing the object with the palm of the hand, in contrast, is more reliable, since the object is trapped between the fingers. Thus, to raise preference for the policy to learn reliable actions, we add observation noise to the object state  $x_i$ , and the object's mass and friction parameters in  $\nu_i$  when generating our data set. Since the loss in Eq. (11) is minimized by actions that achieve low variance in successor state, this will result in our policy selecting actions that achieve the desired push even under uncertainty in the modified physics parameters.

2) *Acquiring a Manipulation State Distribution*: Given the trained policy, we derive a manipulation state distribution parameterized by  $\phi$  by solving

$$\min_{\phi} \mathbb{E}_{x_i^d, x_i, \nu_i} [\mathbb{E}_{x_0} [L_{\theta}(x_0, x_i, \nu_i, x_i^d) \mid x_i, \nu_i, x_i^d, \phi]] \quad (14)$$

over training distributions for  $x_i^d, x_i, \nu_i$ . Here, the inner expected value

$$\mathbb{E}_{x_0} [L_{\theta}(x_0, x_i, \nu_i, x_i^d) \mid x_i, \nu_i, x_i^d, \phi] = \int_{\mathcal{C}_0} L_{\theta}(x_0, x_i, \nu_i, x_i^d) p(x_0 \mid x_i, x_i^d, \nu_i, \phi) dx_0 \quad (15)$$

is the expected loss of the trained policy if we choose initial robot states according to the distribution parameterized by  $\phi$ .

In principle, this expected value would be minimized by a Dirac delta function that places all its probability mass at a robot state that minimizes the loss  $L_{\theta}$  given the arguments  $x_i, x_i^d, \nu_i$ . This, however, is undesirable. The loss  $L_{\theta}$  is defined on a simplified problem that only considers a single object. The state that minimizes  $L_{\theta}$  may not be feasible in the full problem with obstacles that is addressed by the planner. Hence, instead, we opt for a wider distribution that provides the planner with more diverse manipulation state samples. Namely, we choose  $\phi$  to describe an energy-based distribution of the form

$$p(x_0 \mid x_i^d, x_i, \nu_i) = \frac{1}{Z} e^{-\lambda L_{\theta}(x_0, x_i, x_i^d, \nu_i)}, \quad (16)$$

where  $Z$  is a normalization constant and  $\lambda \in \mathbb{R}^+$  a manually selected parameter.

We choose this distribution since its modes are placed on the robot states that allow pushing the object to the desired state in the obstacle-free world. By letting  $\lambda \rightarrow \infty$ , we get a distribution with all its probability mass placed on the minima of  $L_{\theta}$  w.r.t. to the robot state. Vice versa choosing small  $\lambda$ , we get a distribution with wider support, which increases the chance of the distribution to cover the feasible manipulation states of the full problem.

3) *Learning a Generative Model*: The forward models  $f_{\mu}$  and  $f_{\sigma^2}$  allow us to compute  $L_{\theta}$ , and thus the density function in Eq. (16) efficiently. For the QUERYGENERATOR routine in the planner, however, we need to produce samples of robot states following this distribution. We can acquire these using the Markov Chain Monte Carlo (MCMC) method:

$$x_0 \sim p_{\text{MCMC}}(x_0 \mid x_i, x_i^d, \nu_i). \quad (17)$$

This, however, takes several iterations for the distribution to burn in and multiple forward passes through the learned forward models, making this computationally too expensive to be used inside the planner. Hence, instead, we generate a set of samples using this method offline, and train a (conditional) generative adversarial network (GAN) [44] to mimic this distribution online. This way we can generate samples from the distribution with a single forward pass through a neural network.

A GAN consists of two parts: a generator  $G_{\varphi_G}$ , and a discriminator  $D_{\varphi_D}$ . Both are neural networks parameterized by  $\varphi_G$  and  $\varphi_D$  respectively. The generator  $G_{\varphi_G}(x_i, x_i^d, \nu_i, z)$  is a function that maps a random real-valued sample  $z \sim \mathcal{N}(\mathbf{0}, \mathbf{I})$  and its arguments  $x_i, x_i^d, \nu_i$  to a robot state sample. The discriminator outputs the probability that a robot state sample  $x_0$  is drawn from the *true* distribution of manipulation states  $p_{\text{MCMC}}(x_0 \mid x_i, x_i^d, \nu_i)$  that we obtain using MCMC. Both models are trained by solving the following problem:

$$\min_{\varphi_G} \max_{\varphi_D} V(\varphi_D, \varphi_G) \quad (18)$$

with

$$V(\varphi_D, \varphi_G) = \mathbb{E}_{x_0 \sim p_{\text{MCMC}}} [\log(D_{\varphi_D}(x_0, x_i, x_i^d, \nu_i))] + \mathbb{E}_z [\log(1 - D_{\varphi_D}(G_{\varphi_G}(z, x_i, x_i^d, \nu_i), x_i, x_i^d, \nu_i))] \quad (19)$$

On the one hand, this objective trains the discriminator to distinguish between true samples from  $p_{\text{MCMC}}$  and samples generated by the generator. On the other hand, it optimizes the generator to produce samples such that the discriminator can not distinguish these generated samples from the true samples from  $p_{\text{MCMC}}$ . Once learned the generator then serves as an efficient state sampler in the QUERYGENERATOR function.

4) *Summary*: To summarize, the procedure to learn the deterministic policy  $\pi_{\theta}$  and the generator  $G_{\varphi}$  consists of four steps illustrated in Fig. 3 on the left. First, we generate a data set of robot-object interactions using the physics model  $\Gamma$ . Second, we train two forward models  $f_{\mu}$  and  $f_{\sigma^2}$  from this data set under observation noise of the physical properties of the training objects. Third, we use these forward models to compute the loss in Eq. (11) and train the policy  $\pi_{\theta}$ . Fourth, we define an approximate manipulation state distribution according to Eq. (16) and train the generator  $G_{\varphi}$  to imitate samples following this distribution.

## VI. EXPERIMENTS

We implemented and evaluated our approach for robots endowed with configuration spaces in  $SE(2)$ , i.e.  $\mathcal{C}_0 \subseteq SE(2)$ . Evaluating the approach for robots with higher dimensional configuration spaces raises additional challenges that we will

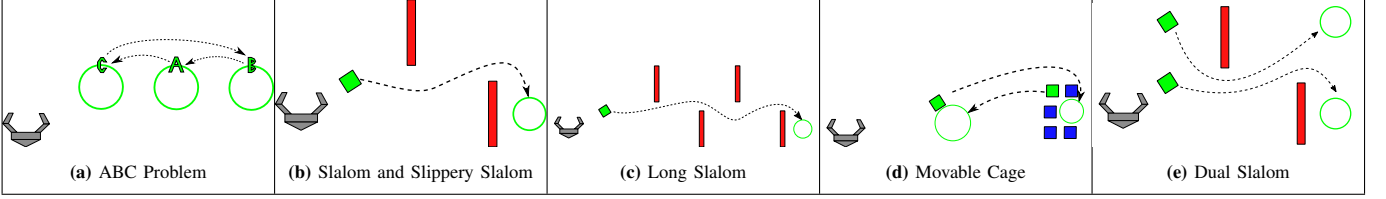


**Fig. 4:** Test scenes for our experiments. These are chosen to test a variety of features: differing object properties, with and without static obstacles, movable obstacles, rearranging single/multiple objects. The scenes Slalom and Slippery Slalom differ in the friction coefficients and mass of the object. In the ABC Problem the objects differ in shape, mass and friction from each other. Green objects are targets  $\mathbf{T}$ , red objects are static obstacles and blue objects are movable objects that are allowed to be moved anywhere, but outside of the planning scene. Consult our online supplementary material for videos of example solutions.

discuss in Sec. VII. For simplicity, we additionally limit our evaluation to holonomic robots. We note though that our approach is not limited to such robots as long as we can efficiently compute a steering function. Unless stated otherwise, we apply in our experiments a planar robot with the geometry of a robotic gripper, as shown in Fig. 4. We choose this geometry because it has interesting properties for the system to learn about.

The action space of all robots in our experiments is the space of bounded translational and rotational velocities applied for some bounded duration:

$$U = \{(v_x, v_y) \in \mathbb{R}^2 \mid v_x^2 + v_y^2 \leq \hat{v}\} \times [-\hat{\omega}, \hat{\omega}] \times [0, \hat{t}]$$

with bounds  $\hat{v}$ ,  $\hat{\omega}$  and  $\hat{t}$ . As the robot is required to be at rest after each action, the actions follow a ramp velocity profile with linear acceleration and deceleration phases similar to [3]. Accordingly, the robot's steering function computes an action that moves the robot on a straight line between two poses ignoring obstacles.

We first present how the robot state generator and policy for this type of robot can be learned. Thereafter, we evaluate these learned models and their performance within the planning algorithm. Additionally, we evaluate how our different design choices in the algorithm affect its planning efficiency.

#### A. Learning Generator and Policy for $SE(2)$ -Robots

1) *Data Generation:* The data set used for training the forward models  $f_\mu$  and  $f_{\sigma^2}$  consists of tuples  $(x_0, x_i, u, x'_0, x'_i, \nu_i)$ . In order for both the generator and the policy to be applicable to different object types, we generate this data for objects  $i$  with different shapes, sizes, mass and friction coefficients. The parameters  $\nu_i$  describing these objects for the generator and policy contain the width and height of the minimal bounding box, the mass and inertia, and the friction coefficient between ground and object. We collect the data by first randomly sampling a robot-object state  $x \in \mathcal{C}_{0:1}$  and an action  $u \in U$ . We then forward propagate these through a stochastic physics model, which we acquire from  $\Gamma$  as described in Sec. V-B1. If the resulting state is valid, i.e. the object comes to rest within a time limit  $T_{\max} = 8s$ , we add the tuple to our data set. Lastly, since the robot's configuration space is also in  $SE(2)$ , we can exploit redundancy in our learning problem. That is, the results of the physical interaction between the robot and the object are translationally and rotationally invariant. Therefore,

we transform all states into a common reference frame such that the robot state is placed at the origin,  $x_0 = 0$ .

2) *Forward Models:* Both forward models  $f_{\sigma^2}$  and  $f_\mu$  are learned with neural networks shown in Fig. 5. The optimization is done using Adam [47] in mini-batches of size 256 for 64,000 steps. The final models are chosen based on validation scores on a held-out validation set. We train both models by maximizing the log-likelihood of a multivariate Gaussian, since the maximum likelihood estimate of normally distributed variables is exactly the mean and the variance. Since we are only interested in the variances, we let the covariance matrix be a diagonal matrix.

3) *Policy:* Based on the learned forward models we can learn the policy  $\pi_\theta$  by minimizing Eq. (11). The architecture of the policy is shown in Fig. 5. The policy is trained in batches from the same data as the forward models. We augment the data tuples  $(x_0, x_i, \nu_i, u, x')$  with object goal states  $x_i^d$  by randomly sampling from a Gaussian over the true successor state  $x'_i$  observed in the data set. The policy is trained for 40,000 steps with the same optimizer and mini-batch size as the forward models.

4) *Generative Model:* The GAN is trained from MCMC samples of robot states. To generate these we first draw samples of initial object and successor states  $x_i, x'_i$  from our data set. These samples are then translated to object frame, i.e. such that  $x_i = 0$ . This simplifies the application of the transition kernel to produce proposal states for the MCMC method. The initial proposals of robot states are drawn from a Gaussian distribution  $\mathcal{N}(0, 0.01^2)$  for the positions, and a uniform distribution  $U(-\pi, \pi)$  for the rotation. Then, new states are proposed by adding Gaussian noise  $\mathcal{N}(0, 0.05^2)$  to the position, and Gaussian noise  $\mathcal{N}(0, 0.5^2)$  to the rotation. Given a current robot state sample  $x_0$ , a new sample  $x'_0$  is accepted by the MCMC method with probability  $\alpha$ , defined as:

$$\alpha = \min(1, e^{\lambda(L_\theta(x_0, x_i, x'_i, \nu_i) - L_\theta(x'_0, x_i, x'_i, \nu_i))}) \quad (20)$$

Here,  $\lambda$  is a temperature parameter that we set in our experiments set to 128. We used a burn-in of 100 iterations and thereafter added the following 300 samples to a data set for training the GAN. In total, we collected  $2 \times 10^6$  MCMC samples for each GAN training.

The architecture of the GAN is shown in Fig. 6. In practice, the GAN objective from Eq. (18) is split up into the following

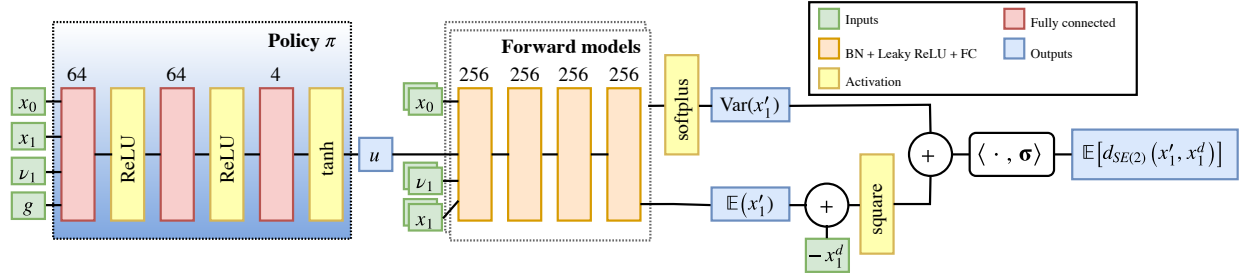


**Fig. 5:** Architecture of forward models and the policy. The forward models are first trained on input tuples  $(x = (x_0, x_1), u, x' = (x'_0, x'_1), \nu)$ . The policy can then be trained by minimizing the rightmost output for randomly sampled desired object states  $x^d_1$ , and back-propagating through the forward models. The forward models are using batch normalization (BN) [45] and leaky ReLUs [46].

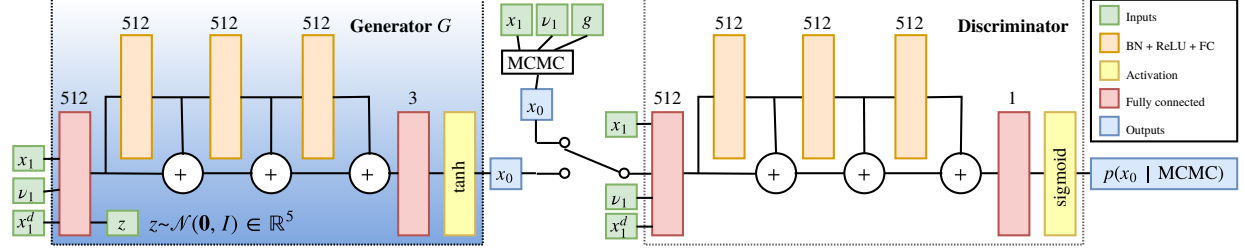


**Fig. 6:** GAN architecture. The generator is trained to mimic the samples that a slower Markov Chain Monte Carlo algorithm provides. Samples can then instead be obtained by a single forward pass of the generator network.

three objectives:

$$\max_{\varphi_G} \mathbb{E}_z [\log(D_{\varphi_D}(G_{\varphi_G}(z, x_i, x^d_i, \nu_i)))] \quad (21)$$

$$\max_{\varphi_D} \mathbb{E}_{x_0 \sim p_{\text{MCMC}}} [\log(D_{\varphi_D}(x_0, x_i, x^d_i, \nu_i))] \quad (22)$$

$$\min_{\varphi_D} \mathbb{E}_z [\log(D_{\varphi_D}(G_{\varphi_G}(z, x_i, x^d_i, \nu_i)))] \quad (23)$$

All three objectives are optimized in mini-batches of size 256 with RMSProp. To stabilize training, the loss in Eq. (23) is trained with probability 0.5 on a batch of generated samples from a replay buffer, and otherwise on a recent batch from the generator. The discriminator is regularized by adding the square of the logits to the loss function. The training is run for 100,000 iterations.

### B. Baselines for Evaluation

To evaluate our algorithm and our learned models, we define several baselines.

1) *Simple Pushing Heuristic*: To evaluate the learned generator and policy, we define a simple generator and policy that share similarities with typical pushing primitives applied in prior rearrangement planning works. To sample a manipulation state, we sample a distance  $r \sim \mathcal{N}(\mu_r, \sigma_r^2)$  and an angle  $\theta \sim \mathcal{N}(0, \sigma_\theta^2)$  for some manually specified  $\mu_r, \sigma_r$  and  $\sigma_\theta$ . The robot is then placed next to the target object at the position  $\mathbf{x}_0 = \mathbf{x}_1 - rR_\theta \frac{\mathbf{x}_1^d - \mathbf{x}_1}{\|\mathbf{x}_1^d - \mathbf{x}_1\|}$ , where  $\mathbf{x}_1, \mathbf{x}_1^d \in \mathbb{R}^2$  are the current and the desired object position, and  $R_\theta \in SO(2)$  a rotation matrix by angle  $\theta$ . The robot's orientation is selected such that its palm faces in the pushing direction. From this robot pose our simple policy steers the robot in a straight line to a position that is offset by the dimensions of the object from the target position  $\mathbf{x}_1^d$ .

2) *HybridActionRRT*: To evaluate our planning algorithm, we compare it to King et al.'s [4] HybridActionRRT algorithm. In brief, this algorithm differs from ours in that it does not structure  $\mathcal{C}_{0:m}$  in slices and applies a different strategy for extending the search tree. The search tree is grown by first randomly sampling a full state  $x^d \in \mathcal{C}_{0:m}$  and then extending the tree from the state that is closest to the sample  $x^d$ . Herein, *closest* is defined by a distance function on  $\mathcal{C}_{0:m}$  that takes the states of all objects and the robot into account. In our experiments, we apply a distance function similar to Eq. (1) with an additional equally weighted term for the distance in robot state.

The EXTENDTREE function of this algorithm samples  $k$  action sequences, where each sequence is either with probability  $p_{\text{rand}}$  sampled uniformly at random or a noisy sample of actions provided by a manipulation primitive. Thereafter, all  $k$  sequences are forward propagated through the physics model and the one that results in a state closest to the random sample  $x^d$  is added to the tree. We equip this algorithm with two manipulation primitives:

- 1 *Transit*: The robot is steered on a straight line from a start state to a goal state.
- 2 *Push*: The robot attempts to push an object  $t$  from a start state to some goal state. To compute such an action, we first use our generator to sample a robot pushing state. Then an action that steers the robot to this state is concatenated with an action provided by our policy for the same state. Note that although this is a similar behavior as in our EXTENDTREE function, the primitive does not propagate these actions through  $\Gamma$ . Hence, any unintended contact that may occur during the approach motion is not considered by this primitive.

For a fair comparison, we evaluate the algorithm for different

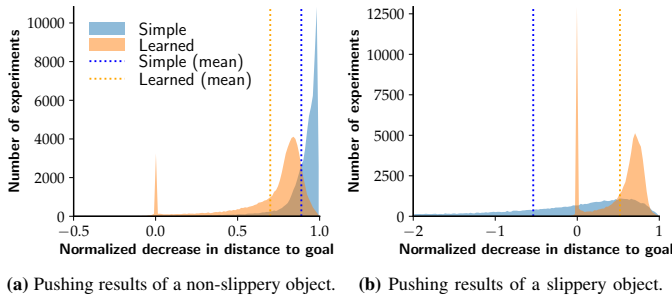


**Fig. 7:** Single push evaluations. We observe the Euclidean distance of an object to a random goal pose before and after executing the policy from a manipulation state. These histograms show the normalized decrease in distances, i.e. the distance after the execution divided by the distance before the execution. The best possible normalized decrease is 1.0. Fig. 7a shows the result for an object that does not slide, whereas Fig. 7b shows results for an object with lower mass and friction that does slide after being pushed.

choices of  $k \in \{1, 4, 8\}$  and  $p_{rand} \in \{0, 0.25, 0.5, 0.75, 1\}$  and select the best. Interestingly, the best performing choice for most test cases is  $k = 1$  and  $p_{rand} = 0.0$ . This indicates that in our test cases there is not much being gained from performing random actions rather than following the *Push* primitive that is based on our policy and generator.

3) *PolicyGeneratorRRT*: To evaluate the effect of the slice-based exploration of our algorithm, we devise a simplified version of our algorithm, *PolicyGeneratorRRT*. This algorithm grows a tree on  $\mathcal{C}_{0:m}$  similar to *HybridActionRRT* without applying the concept of slices. In contrast to *HybridActionRRT*, however, it applies the same *EXTENDTREE* function as our algorithm. Hence, the main difference to *HybridActionRRT* with the primitives defined above is that an approach *transit* and a following pushing action are propagated separately through  $\Gamma$ . This allows the policy to be applied to the resulting state of the *transit* action, i.e. it allows the policy, to some extent, to adapt to unintended contact during the approach motion.

### C. Technical Details

We implemented the planning algorithms in C++ using OMPL [48]. Similarly, the simple generator and policy were also implemented in C++. The learned generator and the learned policy in contrast were implemented in Python using PyTorch. The communication between these and the planner was performed using Protobuf. The overhead of this communication is not included in our evaluation. As physics model we chose Box2D [32]. All experiments were run on Ubuntu 14.04 on an Intel(R) Core(TM) i7-3770 CPU@3.40GHz with 32GB RAM.

### D. Evaluation of Policy and Generator

1) *Quantitative Evaluation*: To evaluate our learned models, we compare their performance in transporting a single object with that of the simple heuristic. Our evaluation procedure follows the extension strategy of our planning algorithm. Given an initial state of the object and a randomly sampled target state, we first place the robot in a manipulation state produced by the generator. Next, we query the policy to provide a single action to transport the object towards the goal

state and forward propagate this through the physics model  $\Gamma$ . We then compare the Euclidean distance between the resulting object state and the goal state.

Fig. 7 shows the results of this procedure for two different box-shaped objects that differ in mass and friction. One box is slippery, i.e. it does not immediately come to rest after being pushed, and one box is non-slippery. In case of the non-slippery box, we observe that both the learned and the simple models on average succeed at transporting the object towards the target position. Although the learned models on average reduce the distance by more than half, the simple models are yet better in this case. For the slippery object, in contrast, the learned models are significantly better than the simple ones. Here, the learned models achieve similar results as in the non-slippery case, whereas the simple heuristic often results in a significant increase in distance. This highlights a weakness of such simple hand-made heuristics. A behavior that works well for some types of objects may not work well for others. The learned models, on the other hand, are parameterized by the expected physical properties of the object and can thus adjust their behavior. Achieving similar results with hand-made heuristics would require significant engineering efforts.

2) *Qualitative Evaluation*: Next, we qualitatively evaluate the learned generator. Fig. 8 shows robot state samples produced by learned generators for two different robots. Fig. 8a shows these samples for our gripper-shaped robot and Fig. 8b shows these for a robot consisting of two small squares. In both cases, the generators learned how the robot should be positioned relative to the object in order to push it in some desired direction. More interestingly, however, is that in both cases it also learned a preference in orientation of the robot. In the case of the gripper, it prefers orientations such that the object is placed between the gripper’s fingers. In case of the two-point robot, it prefers orientations for which the robot achieves two-point-contacts with the object. In both cases, these choices lead to pushing behaviors that are more robust against uncertainty in object properties than pushing from other orientations.

As can be seen, the samples show that the generators learned distributions with a wide support over several possible manipulation states. This is particularly useful, if some of these states are in collision or can not be approached easily in the presence of obstacles. In particular for the gripper-shaped robot, the generator learned states where the robot is facing perpendicular to the direction of transport. Accordingly, the actions learned by the policy in these states, move the robot sideways. Note that this is a behavior that makes specific use of the robot’s geometric properties, i.e. its fingers. One drawback of these wide distributions, however, is that there may also be a small probability to sample distant states from which transporting the object within one action is not possible. Such states are responsible for the cases in Fig. 7 where the distance to the goal is not decreased at all.

### E. Evaluation of the Planning Algorithm

Next, we evaluate the effects of our different algorithm design choices as well as how the learned models compare to

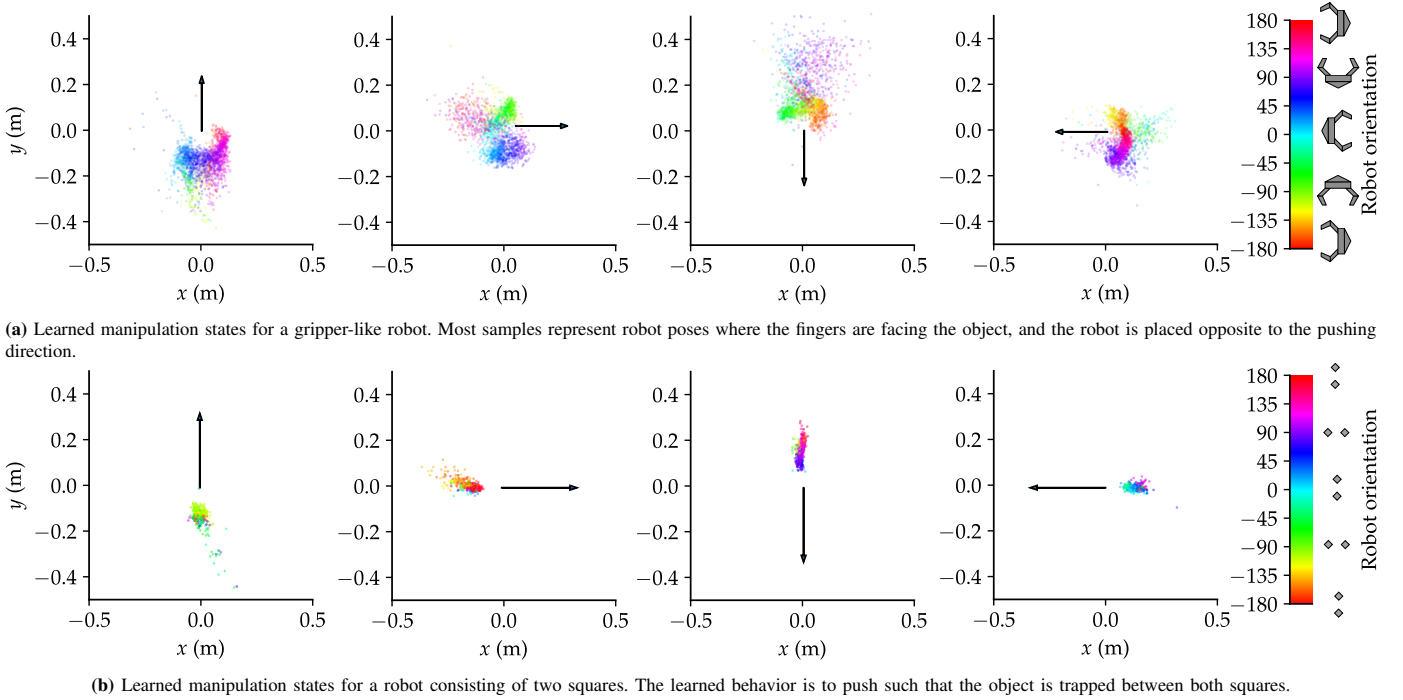


**Fig. 8:** Samples of robot states from our generative adversarial network. The arrow represents a desired push of an object starting in the origin. Each colored dot represents a robot position, where the color is the rotation of the robot. Consult our online supplementary material for a video showing how the samples are influenced by different arguments to the generator.

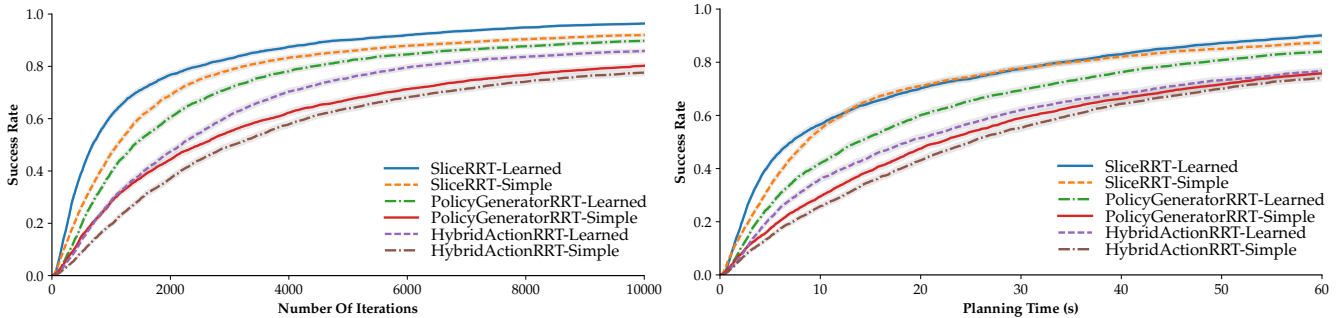


**Fig. 9:** Planning success rate as function of number of iterations (*left*) and planning time (*right*). For any given number of iterations  $n$ , the corresponding success rate can be interpreted as an empirically determined probability that an algorithm successfully finds a solution within  $n$  iterations. The shaded areas show the 95% Wilson confidence interval of this probability. After a total of 180s the ratio of successful planning instances was: SliceRRT-Learned: 99.2%, SliceRRT-Simple: 96.6%, PolicyGeneratorRRT-Learned: 95.2%, PolicyGeneratorRRT-Simple: 91.9%, HybridActionRRT-Learned: 92.2%, HybridActionRRT-Simple: 91.2%. For SliceRRT and PolicyGeneratorRRT we chose  $p_{rand} = 0.01$ .

the simple ones when used in a planner. In the comparisons with our baselines, we refer to our algorithm by the name SliceRRT.

*1) Overall Performance:* We run all three algorithms with both the learned policy and generator as well as the simple ones on six different scenes shown in Fig. 4. We run each algorithm-policy-generator combination for 640 times on each scene and record the runtime, the number of iterations and whether the algorithm succeeds at finding a solution within a time budget of 180s.

The planning success rates as a function of number of iterations are shown in Fig. 9 on the left. As the number of iterations increases, more planning instances terminate successfully and the success rates tend towards 1. Our SliceRRT algorithm achieves with both policy-generator models the steepest initial increase as well as the highest success rates after the first

10,000 iterations. The curves for both PolicyGeneratorRRT and HybridActionRRT are significantly flatter for both the learned policy and generator as well as the simple ones. Overall, the success rates remain below the one of SliceRRT. It is notable that for each algorithm the learned policy and generator outperform the simple ones.

Similarly, the success rate as a function of planning time is shown on the right of Fig. 9 for the first 60s. Also here SliceRRT with learned policy and generator achieves the steepest initial increase and highest final success rate. The difference, however, between the simple and the learned policy and generator is smaller due to increased computational costs of the learned models. We note, however, that this effect also depends on implementation details. Overall, these results indicate that:

1. The learned policy and generator provide better guidance



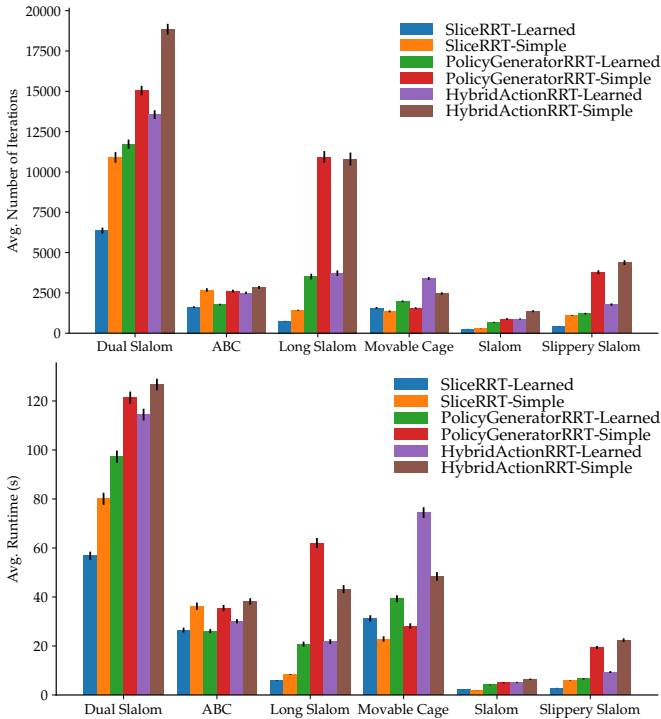


Fig. 10: Average number of iterations (*top*) and average runtime (*bottom*) per algorithm-policy-generator pair per tested scene.

than the simple ones;

2. SliceRRT is more efficient in terms of iterations and runtime on the tested problems than the other algorithms.

In particular, the poorer performance of PolicyGeneratorRRT shows that the slice-based exploration increases the algorithm’s efficiency significantly.

2) *Performance per Scene*: Next, we investigate how the average runtime differs per test scene, see Fig. 10. For all algorithms we observe for most scenes better or similar results for the learned policy and generator than for the simple ones. The differences between the learned and the simple models are most significant on Dual Slalom, ABC, Long Slalom and Slippery Slalom. This confirms our observations from Sec. VI-D as all of these scenes contain at least one object with low friction and low mass.

The best results on most scenes are achieved by SliceRRT with learned policy and generator. The differences are particularly strong on the different slalom scenes. In these scenes the robot and the objects can potentially be very distant and separated by static obstacles. It appears that the slice-based exploration has its strongest benefit in these situations. The differences between PolicyGeneratorRRT and HybridActionRRT are not as significant for many scenes. Most notably is the difference for Movable Cage, where we have many movable objects, which are initially close to each other. In such a situation it is likely that the target object is moved through direct or indirect contact when approaching a manipulation state. HybridActionRRT, in contrast to PolicyGeneratorRRT, queries the policy before propagating the approach motion to the manipulation state. Choosing a pushing action given an updated state, as in PolicyGeneratorRRT, seems in this case to be most beneficial.

## VII. DISCUSSION AND CONCLUSION

The goal of this work was to design an efficient algorithm that can solve non-prehensile MAMO and rearrangement problems, while making few limiting assumptions on the robot’s manipulation abilities. For this, we presented an algorithm based on the kinodynamic RRT algorithm that explores the composite configuration space  $\mathcal{C}_{0:m}$  of robot and objects. The algorithm is agnostic to the robot’s manipulation abilities by modeling the effects of robot-centric actions through a dynamic physics model  $\Gamma$ . It achieves efficiency by segmenting the search space into slices of similar object arrangements, and deploying a learned pushing policy and robot state generator for guidance. The slice segmentation allows the planner to select the most suitable states from its search tree to extend towards a desired object arrangement. The learned robot state generator provides the planner with robot states from which pushing an object in a desired direction is possible. Similarly, the learned policy provides the planner with robot actions achieving these pushes. Our experiments demonstrate that our approach can successfully compute rearrangement solutions for various scenes without a human designer explicitly modeling the robots manipulation abilities. Furthermore, all techniques together allow our algorithm to explore its search space more efficiently than a comparable approach, leading to lower average planning times.

### A. Slice-based Exploration

The slice-based exploration structures the search and has several benefits over a purely state-based exploration as applied in [2]–[4]. First, when selecting a state for extension, it naturally takes into account that the planner operates on different subspaces of  $\mathcal{C}_{0:m}$ . For many robots it is simpler to steer the robot between different states within a slice than to compute actions that move objects between slices. In a purely state-based approach, such as HybridActionRRT, this needs to be expressed through a weighting factor that balances between robot and object state distances when selecting a nearest neighbor. In contrast, our slice-segmentation naturally reflects the difference between both types of states and alleviates us from tuning such a weighting factor.

Second, the algorithm balances its effort on exploring *transit* actions within the different slices in a meaningful manner. The subset  $\mathcal{T} \cap s$  of explored states that lie within the same slice  $s$  form a sub-RRT for this slice<sup>1</sup>. This sub-RRT fulfills the task of classical robot path planning given the object arrangement in  $s$ . It is extended every time  $s$  is selected and either expanded towards a uniformly sampled ( $t = 0$ ) or a manipulation state ( $t \neq 0$ ). The probability of this extension to occur is proportional to the measure of the Voronoi region of  $s$  w.r.t.  $d_s$  in  $\mathcal{S}$ . Hence, the algorithm spends more time on exploring robot states within slices for which not many neighboring object arrangements have been reached than for others.

<sup>1</sup>In principle,  $\mathcal{T} \cap s$  may consist of several disjoint connected components. This can occur if the robot first leaves the slice  $s$  through a *transfer* action but later on enters the slice again through another *transfer* action that places the moved objects back to their original poses. We note, however, that this is highly unlikely to occur.



### B. Forward Propagation through Physics Model

As a physics-based approach, our approach shifts most assumptions on the manipulation abilities of the robot and the mechanics of manipulation into the model  $\Gamma$ . Treating this model as a black box has the benefit that it can be replaced with any physics model. In our implementation we chose a rigid body physics simulator for this. Alternatively, we could also choose, for instance, a learned model. Assuming that  $\Gamma$  is deterministic, however, implicitly assumes perfect knowledge about the manipulated objects. In general, this is not feasible for a robot operating in a real environment. As a consequence, solutions planned by our planner have high chance of failure when executed on a real system due to inaccurate predictions of  $\Gamma$ .

In the context of physics-based manipulation planning, this issue has recently been addressed by several works [49]–[51]. Koval et al. [50] present a multi-arm-bandit-based meta-planner that selects the solution that is most robust against model uncertainties from a set of solutions computed by a planner similar to ours. King et al. [51] present a Monte-Carlo-Tree-Search-based algorithm that plans robust non-prehensile MAMO solutions on belief space. In both works, our planner could be applied as a primitive.

In future work, we intend to investigate how uncertainty in  $\Gamma$  can be addressed further. Here, we believe learning a pushing policy that is robust and provides uncertainty reducing actions could be highly beneficial.

### C. Learning Pushing State Generator and Policy

Learning the pushing state generator and policy from data generated using the physics model has several advantages. First, retraining these allows an easy adaptation of the planner to different robot embodiments and new object types. Second, we do not impose any unnecessary restrictions on the robot’s manipulation abilities. Third, both generator and policy can be parameterized by expected physical properties of the objects and trained such that the learned pushing behavior is robust against uncertainty in these quantities.

Training both policy and state generator for any robot, however, is challenging. Our current approach to collecting training data has only been evaluated for robots with configuration spaces in  $SE(2)$ . Due to the uniform random sampling, the procedure is limited to robots with configuration and action spaces for which the probability of sampling a robot state and action that pushes the target object is non-zero. For robots with high degrees of freedom, e.g. a 7-DoF manipulator, sampling such state-action pairs may either have zero or very low probability. Hence, for such robots a more sophisticated data acquisition is required. In future work, we plan to investigate this and extend our approach to robot manipulators. Learning a pushing policy and state generator for such robots is particularly interesting as it would allow the planner to purposefully utilize full-arm pushing actions that are difficult to model otherwise.

We trained our pushing policy and generator to push a single object at a time. While this doesn’t restrict the planner to apply actions that push multiple objects at once, learning a policy

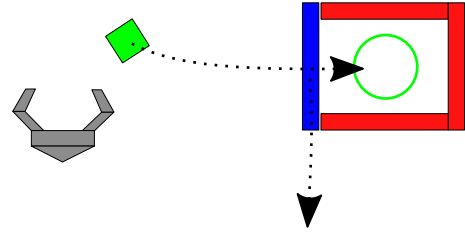


**Fig. 11:** A problem with a narrow passage in object arrangement. To solve this problem the robot needs to push the blue object downwards and then push the green box into the goal region.

and a state generator for such multi-object pushing actions might be beneficial. Another limitation of our current policy is its precision. While it on average succeeds at reducing the distance to a desired state, it does not succeed in reaching it exactly. In particular pushing an object towards a desired orientation proved to be difficult for the trained policy.

Instead of training a one-step policy, we could alternatively integrate a multi-step policy that operates as a closed-loop controller running in the physics model. While this would likely improve the accuracy of pushing actions, the additional computational overhead could prove disadvantageous. In preliminary experiments, we equipped the algorithm with a local planner for *transit* actions that attempts to avoid collisions when approaching a manipulation state. This version of our algorithm, however, performed worse than the evaluated one that only applies straight line steering for the robot. This indicates that there is a fundamental trade-off between the versatility and computational overhead of local planners in the algorithm.

### D. Challenging Rearrangement Problems

A major challenge in rearrangement planning arises from the need to clear obstructions. Consider the problem shown in Fig. 11, where the robot first needs to push an obstacle aside to push its target object to the goal. The directions in which this obstacle can be pushed are very limited due to the static obstacles (red). In other words, a solution to this problem needs to pass through a narrow passage of object arrangements, which has low probability to be sampled.

As a sampling-based approach, our planner struggles with scenarios like this. A higher level logic is required that replaces the uniform slice sampling with a more sophisticated mechanism. The challenge here lies in formulating such a logic without making strong assumptions on the robot’s manipulation abilities. The question whether an object is obstructed by another depends not only on the objects and their states, but also on the robot’s embodiment. Hence, we see a potential line of future work in learning a high level policy that is conditioned on the robot’s actual manipulation abilities and directs the search to solve more challenging rearrangement problems.

## APPENDIX

### A. Online Supplementary Material

Supplementary material is available online on [https://joshuahaustein.github.io/learning\\_rearrangement\\_planning/](https://joshuahaustein.github.io/learning_rearrangement_planning/). The website contains videos of example solutions

computed by our planner, as well as a video illustrating the extension strategy of our algorithm when using the generator and policy. Additionally, the website contains videos that show how the learned policy and generator behave for different arguments, such as different physical parameters of the target object and different target states.

## REFERENCES

- [1] A. Cosgun, T. Hermans, V. Emeli, and M. Stilman, "Push planning for object placement on cluttered table surfaces," *Proceedings - IEEE International Conference on Intelligent Robots and Systems*, pp. 4627–4632, Sept 2011.
- [2] J. E. King, J. A. Haustein, S. S. Srinivasa, and T. Asfour, "Nonprehensile whole arm rearrangement planning on physics manifolds," *Proceedings - IEEE International Conference on Robotics and Automation*, pp. 2508–2515, June 2015.
- [3] J. A. Haustein, J. King, S. S. Srinivasa, and T. Asfour, "Kinodynamic randomized rearrangement planning via dynamic transitions between statically stable states," *Proceedings - IEEE International Conference on Robotics and Automation*, pp. 3075–3082, June 2015.
- [4] J. E. King, M. Cagnetti, and S. S. Srinivasa, "Rearrangement planning using object-centric and robot-centric action spaces," *Proceedings - IEEE International Conference on Robotics and Automation*, pp. 3940–3947, May 2016.
- [5] M. Stilman, J. U. Schamburek, J. Kuffner, and T. Asfour, "Manipulation planning among movable obstacles," *Proceedings - IEEE International Conference on Robotics and Automation*, pp. 3327–3332, April 2007.
- [6] M. R. Dogar and S. S. Srinivasa, "A planning framework for non-prehensile manipulation under clutter and uncertainty," *Autonomous Robots*, vol. 33, no. 3, pp. 217–236, October 2012.
- [7] G. Wilfong, "Motion planning in the presence of movable obstacles," *Annals of Mathematics and Artificial Intelligence*, vol. 3, no. 1, pp. 131–150, March 1991.
- [8] T. S. Rachid Alami, Jean-Paul Laumond, "Two manipulation planning algorithms," in *Proceedings - Workshop on Algorithmic Foundations of Robotics*, 1994.
- [9] O. Ben-Shahar and E. Rivlin, "Practical pushing planning for rearrangement tasks," *IEEE Transactions on Robotics and Automation*, vol. 14, no. 4, pp. 549–565, 1998.
- [10] J. Ota, "Rearrangement of multiple movable objects - integration of global and local planning methodology," *Proceedings - IEEE International Conference on Robotics and Automation*, pp. 1962–1967, 2004.
- [11] J. Scholz and M. Stilman, "Combining motion planning and optimization for flexible robot manipulation," *Proceedings - IEEE-RAS International Conference on Humanoid Robots*, pp. 80–85, December 2010.
- [12] A. Krontiris and K. Bekris, "Dealing with Difficult Instances of Object Rearrangement," *Proceedings - Robotics: Science and Systems*, July 2015.
- [13] A. Krontiris and K. E. Bekris, "Efficiently solving general rearrangement tasks: A fast extension primitive for an incremental sampling-based planner," *Proceedings - IEEE International Conference on Robotics and Automation*, pp. 3924–3931, May 2016.
- [14] C. R. Garrett, T. Lozano-Pérez, and L. P. Kaelbling, "FFRob: Leveraging symbolic planning for efficient task and motion planning," *International Journal of Robotics Research*, vol. 37, no. 1, pp. 104–136, 2018.
- [15] J. Barry, K. Hsiao, L. P. Kaelbling, and T. Lozano-Pérez, "Manipulation with Multiple Action Types," *Proceedings - International Symposium on Experimental Robotics*, pp. 531–545, June 2012.
- [16] G. Havur, G. Ozbilgin, E. Erdem, and V. Patoglu, "Geometric rearrangement of multiple movable objects on cluttered surfaces: A hybrid reasoning approach," *Proceedings - IEEE International Conference on Robotics and Automation*, pp. 445–452, May 2014.
- [17] S. Jentzsch, A. Gaschler, O. Khatib, and A. Knoll, "MOPL: A multi-modal path planner for generic manipulation tasks," *Proceedings - IEEE International Conference on Intelligent Robots and Systems*, pp. 6208–6214, September 2015.
- [18] M. Stilman and J. J. Kuffner, "Navigation among movable obstacles: real-time reasoning in complex environments," *International Journal of Humanoid Robotics*, vol. 02, no. 04, pp. 479–503, December 2005.
- [19] J. van den Berg, M. Stilman, J. Kuffner, M. Lin, and D. Manocha, "Path planning among movable obstacles: A probabilistically complete approach," *Algorithmic Foundation of Robotics VIII: Selected Contributions of the Eight International Workshop on the Algorithmic Foundations of Robotics*, pp. 599–614, 2010.
- [20] D. Nieuwenhuisen, A. F. Van Der Stappen, and M. H. Overmars, "An effective framework for path planning amidst movable obstacles," *Algorithmic Foundation of Robotics VII: Selected Contributions of the Seventh International Workshop on the Algorithmic Foundations of Robotics*, vol. 47, pp. 87–102, 2008.
- [21] O. Ben-Shahar and E. Rivlin, "To push or not to push: on the rearrangement of movable objects by a mobile robot," *IEEE Transactions on Systems, Man and Cybernetics, Part B (Cybernetics)*, vol. 28, no. 5, pp. 667–679, 1998.
- [22] T. Siméon, J. P. Laumond, J. Cortés, and A. Sahbani, "Manipulation planning with probabilistic roadmaps," *International Journal of Robotics Research*, vol. 23, no. 7-8, pp. 729–746, August 2004.
- [23] A. Krontiris, R. Shome, A. Dobson, A. Kimmel, and K. Bekris, "Rearranging similar objects with a manipulator using pebble graphs," *Proceedings - IEEE-RAS International Conference on Humanoid Robots*, pp. 1081–1087, November 2015.
- [24] S. M. LaValle, *Planning Algorithms*. Cambridge University Press, 2006.
- [25] K. Hauser, "The minimum constraint removal problem with three robotics applications," *The International Journal of Robotics Research*, vol. 33, no. 1, pp. 5–17, Jan 2014.
- [26] M. R. Dogar and S. S. Srinivasa, "Push-grasping with dexterous hands: Mechanics and a method," *Proceedings - IEEE/RSJ International Conference on Intelligent Robots and Systems*, pp. 2123–2130, October 2010.
- [27] J. Barry, L. P. Kaelbling, and T. Lozano-Pérez, "A hierarchical approach to manipulation with diverse actions," *Proceedings - IEEE International Conference on Robotics and Automation*, pp. 1799–1806, November 2013.
- [28] K. M. Lynch and M. T. Mason, "Stable pushing: Mechanics, controllability, and planning," *International Journal of Robotics Research*, vol. 15, no. 6, pp. 533–556, December 1996.
- [29] D. Nieuwenhuisen, A. van der Stappen, and M. Overmars, "Path planning for pushing a disk using compliance," *Proceedings - IEEE/RSJ International Conference on Intelligent Robots and Systems*, pp. 714–720, August 2005.
- [30] J. Zhou and M. T. Mason, "Pushing revisited: Differential flatness, trajectory planning and stabilization," *Proceedings - International Symposium on Robotics Research (ISRR)*, December 2017.
- [31] E. Coumans, "Bullet physics library," <https://pybullet.org>, (accessed April 2018).
- [32] E. Catto, "Box2d," <http://box2d.org>, 2010 (accessed April 2018).
- [33] R. Smith, "Open Dynamics Engine," <http://www.ode.org>, 2000 (accessed April 2018).
- [34] E. Todorov, T. Erez, and Y. Tassa, "Mujoco: A physics engine for model-based control," *Proceedings - IEEE/RSJ International Conference on Intelligent Robots and Systems*, pp. 5026–5033, October 2012.
- [35] C. Zito, R. Stolkin, M. Kopicki, and J. L. Wyatt, "Two-level RRT planning for robotic push manipulation," *Proceedings - IEEE International Conference on Intelligent Robots and Systems*, pp. 678–685, October 2012.
- [36] N. Kitaev, I. Mordatch, S. Patil, and P. Abbeel, "Physics-based trajectory optimization for grasping in cluttered environments," *Proceedings - IEEE International Conference on Robotics and Automation*, pp. 3102–3109, May 2015.
- [37] S. M. LaValle and J. J. Kuffner, "Randomized kinodynamic planning," *International Journal of Robotics Research*, vol. 20, no. 5, pp. 378–400, May 2001.
- [38] S. Elliott, M. Valente, and M. Cakmak, "Making objects graspable in confined environments through push and pull manipulation with a tool," *Proceedings - IEEE International Conference on Robotics and Automation*, pp. 4851–4858, May 2016.
- [39] Z. Wang, S. Jegelka, L. P. Kaelbling, and T. Lozano-Pérez, "Focused model-learning and planning for non-Gaussian continuous state-action systems," *Proceedings - IEEE International Conference on Robotics and Automation*, pp. 3754–3761, May 2017.
- [40] C. G. Atkeson and J. C. Santamaria, "A comparison of direct and model-based reinforcement learning," *Proceedings - IEEE International Conference on Robotics and Automation*, pp. 3557–3564, April 1997.
- [41] C. Finn and S. Levine, "Deep visual foresight for planning robot motion," *Proceedings - IEEE International Conference on Robotics and Automation*, pp. 2786–2793, May 2017.
- [42] M. Andrychowicz, D. Crow, A. Ray, J. Schneider, R. Fong, P. Welinder, B. McGrew, J. Tobin, O. P. Abbeel, and W. Zaremba, "Hindsight experience replay," *Proceedings - Advances in Neural Information Processing Systems*, pp. 5055–5065, December 2017.

- [43] D. Silver, G. Lever, N. Heess, T. Degris, D. Wierstra, and M. Riedmiller, "Deterministic policy gradient algorithms," *Proceedings - International Conference on Machine Learning*, pp. 1–387–I–395, June 2014.
- [44] I. Goodfellow, J. Pouget-Abadie, M. Mirza, B. Xu, D. Warde-Farley, S. Ozair, A. Courville, and Y. Bengio, "Generative adversarial nets," *Proceedings - Advances in Neural Information Processing Systems*, pp. 2672–2680, December 2014.
- [45] S. Ioffe and C. Szegedy, "Batch normalization: Accelerating deep network training by reducing internal covariate shift," *Proceedings - International Conference on Machine Learning*, pp. 448–456, July 2015.
- [46] A. L. Maas, A. Y. Hannun, and A. Y. Ng, "Rectifier nonlinearities improve neural network acoustic models," *International Conference on Machine Learning - Workshop on Deep Learning for Audio, Speech, and Language Processing*, June 2013.
- [47] D. Kingma and J. Ba, "Adam: A method for stochastic optimization," *Proceedings - International Conference on Learning Representations*, 2015.
- [48] I. A. Şucan, M. Moll, and L. E. Kavraki, "The Open Motion Planning Library," *IEEE Robotics & Automation Magazine*, vol. 19, no. 4, pp. 72–82, December 2012.
- [49] A. M. Johnson, J. King, and S. Srinivasa, "Convergent planning," *IEEE Robotics and Automation Letters*, vol. 1, no. 2, pp. 1044–1051, July 2016.
- [50] M. C. Koval, J. E. King, N. S. Pollard, and S. S. Srinivasa, "Robust trajectory selection for rearrangement planning as a multi-armed bandit problem," *Proceedings - IEEE International Conference on Intelligent Robots and Systems*, pp. 2678–2685, September 2015.
- [51] J. E. King, V. Ranganeni, and S. S. Srinivasa, "Unobservable Monte Carlo planning for nonprehensile rearrangement tasks," *Proceedings - IEEE International Conference on Robotics and Automation*, pp. 4681–4688, May 2017.